Appendix 7-6: Status of the Atmospheric Dispersion and Deposition Model

EPA to model atmospheric dispersion and deposition to the Everglades. As discussed in Chapter 7, DEP has recently undertaken a pilot project to determine the technical feasibility and information requirements for defining a Total Maximum Daily Load (TMDL) for atmospheric mercury for the Everglades. The Dispersion and Deposition Model is fundamental to any attempt to control mercury in the Everglades. For the TMDL pilot project, University of Michigan Air Quality Laboratory prepared the report which follows.

Project Final Technical Report

Modeled Deposition of Speciated Mercury to the SFWMD Water Conservation Area 3A: 22 June 1995 to 21 June 1996

Project Description and Results

Submitted by:

Gerald J. Keeler, Frank J. Marsik, Khalid I. Al-Wali and J. Timothy Dvonch

THE UNIVERSITY OF MICHIGAN AIR QUALITY LABORATORY
Ann Arbor, Michigan 48109

TABLE OF CONTENTS

1. Project Summary

Event-based precipitation samples were collected at a site in Davie, Florida for a one-year period (22 June 1995 to 21 June 1996) in an effort to obtain a better understanding of the daily variability in mercury wet-deposition (Dvonch 1998). The temporal variation in the wet-deposition at that the Davie site during the one-year period is presented in Figure 1.

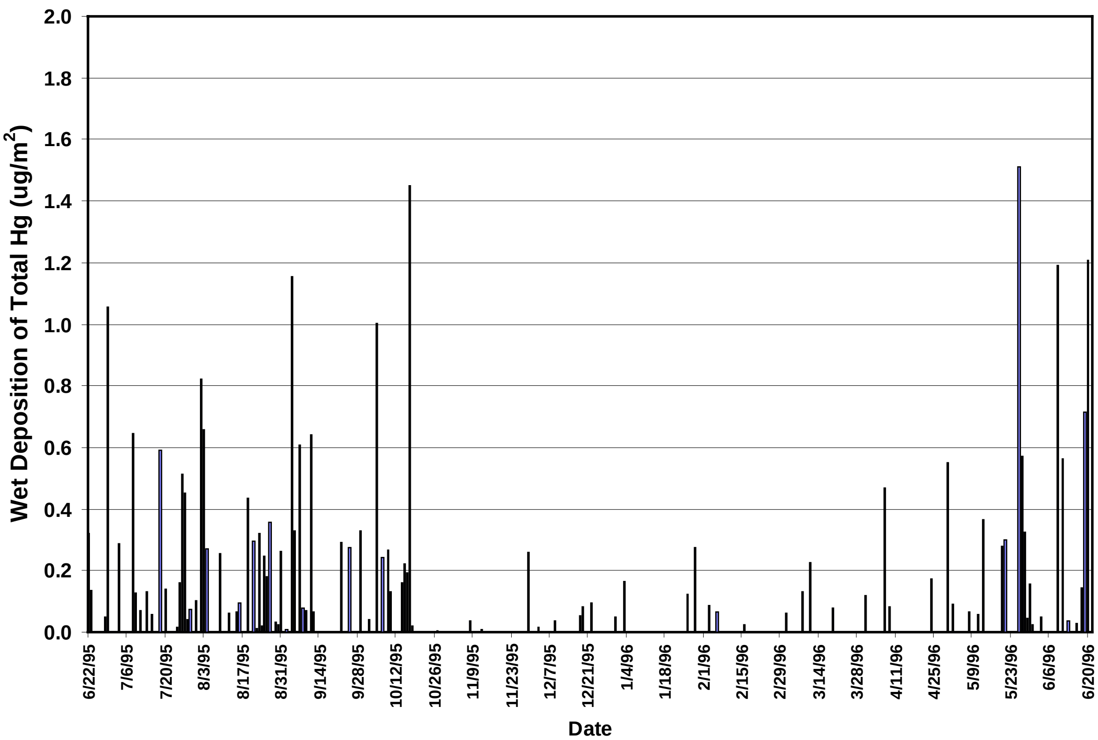

Figure 1. Temporal variation in event wet-deposition of total mercury at Davie, Florida for the period 22 June 1995 to 21 June 1996.

A seasonal pattern in mercury wet-deposition can clearly been seen, with elevated levels of deposition associated with the climatological "wet season" in South Florida, typically May through October. Analysis of the one-year database indicated that differences in observed rainfall depth accounted for 14 % of the variability in observed event mercury concentration at the Davie site (Dvonch 1998). Past studies investigating acid wet-deposition at other locations have noted that considerable variability in observed precipitation chemistry (10 to 40%) could be attributed to differences in the atmospheric transport regimes impacting a given site. Thus, a hybrid modeling study was conducted to understand the potential impact of such varying transport regimes on the wet-deposition of total mercury at the Davie site and across South Florida. This hybrid modeling approach employed a Lagrangian transport/dispersion model, a statistical model and a mesoscale meteorological model to obtain annual estimates of the wet- and dry-deposition of total mercury to South Florida. The final results of the project are being prepared for submission to the Journal of Applied Meteorology (Marsik *et al*., *In Preparation*).

The current study builds upon the results of the previous study and uses the same hybrid modeling approach to obtain estimates of the monthly and annual wet- and dry-deposition of speciated mercury [Hg(0), Hg(II) and Hg(p)] to the South Florida Water Management District's Water Conservation Area 3 (SFWMD WCA3) during the same one-year period used for the previous study (22 June 1995 to 21 June 1996). Modeling was performed for three different mercury emissions "scenarios" in an effort to better understand the potential impact of uncertainties in the current mercury emissions inventory. Our BASE CASE scenario characterizes emissions based upon the emissions inventory used in the USEPA Mercury Study Report to Congress (US EPA 1997). The two additional scenarios modeled in this current project used modified emissions inventories based upon the work of Dvonch *et al*. (1999).

Using our hybrid approach, it was determined that South Florida was impacted by eight different atmospheric transport regimes (or clusters) during the period studied, each representing a particular synoptic meteorological flow regime. Representative days from each transport regimes (or clusters) were modeled and average deposition patterns and estimates were obtained for each cluster. Finally, monthly and annual estimates were calculated by weighting the cluster average deposition amounts by their frequency of occurrence, resulting in annual total mercury wet- and dry-deposition fluxes to the SFWMD WCA3. Using the BASE CASE emissions inventory, the modeling results for the year studied suggest a total mercury wet-deposition to SFWMD WCA3 of 18.74 ± 6.15 $\mu g/m^2$/year, with the annual speciated wet-deposition estimated to be 0.01 ± 0.00 $\mu g/m^2$ for Hg(0), 14.40 ± 4.51$\mu g/m^2$ for Hg(II) and 4.33 ± 1.65 $\mu g/m^2$ for Hg(p). The greatest monthly total mercury wet-deposition was estimated for the month of July 1995, 3.98 ± 0.61 $\mu g/m^2$. Dry-deposition modeling results suggested an annual total mercury dry-deposition of 12.20 ± 7.4 $\mu g/m^2$/year, with the annual speciated dry-deposition estimated to be 0.06 $\mu g/m^2$ for Hg(0), 11.20 ± 6.80 $\mu g/m^2$ for Hg(II) and 0.94 ± 0.53 $\mu g/m^2$ for Hg(p). The greatest monthly total mercury dry-deposition was estimated for the month of September 1995, 1.29 ± 0.72 $\mu g/m^2$. Seasonal trends were noted for both total mercury wet- and dry-deposition.

2. Methodology and model descriptions

As noted in the previous section, this project employed a hybrid modeling approach to obtain estimates of the monthly and annual wet- and dry-deposition of speciated mercury [Hg(0), Hg(II) and Hg(p)] to the South Florida Water Management

District's Water Conservation Area 3 (SFWMD WCA3). The specific steps employed in this hybrid approach are as follows:

(1) Compute daily back-trajectories (ending in Davie, FL) for each day of a one-year period (22 June 1995 to 21 June 1996). This year was chosen as precipitation was collected on an event (i.e., daily) basis at the University of Florida Agricultural Station in Davie, FL.

(2) Identify meteorologically-based clusters that represent the dominant atmospheric transport regimes that impacted South Florida during the one-year study period.

(3) Select a number of representative days from each cluster and use a mesoscale meteorological model to obtain three-dimensional meteorological fields (U and V wind components, vertical velocity, temperature, specific humidity and pressure) for the selected representative days.

(4) Using the meteorological fields computed in part (3) as input fields, use a Lagrangian air-pollution dispersion/deposition model to estimate average wet- and dry-deposition patterns/amounts for each of these representative days, computing a cluster average deposition for each of the clusters.

(5) Weight the average daily wet- and dry-deposition estimates for each cluster by the number of days assigned to each cluster, and thus obtain an estimate of the speciated monthly and annual wet- and dry-depositional loading of mercury to the SFWMD WCA3.

The tools used to perform the above tasks are outlined below:

a. Determination of 72-hour back-trajectories

Daily back-trajectories were computed using the HYbrid Single Particle Lagrangian Integrated Trajectories Model Version 4 (HYSPLIT_4) (Draxler and Hess, 1997). HYSPLIT_4 is a complete modeling system that can be used for a range of meteorological/air quality applications ranging from the calculations of simple forward- and/or backward-trajectories to the performance of complex dispersion/deposition simulations. The initial version of the model (Draxler and Taylor, 1982) used rawinsonde observations as the meteorological input data and the dispersion calculations performed with the model assumed uniform mixing during the daytime and no mixing during the nighttime. In time, the model was updated to include the use of gridded meteorological data from either analyses or short-term forecasts as input data, and was updated to include the use of a temporally and spatially varying diffusivity profile for use in the dispersion and deposition calculations.

For this study, the input data used for the calculation of the daily back-trajectories consisted of analysis and short-term forecasted meteorological fields from the National Center for Environmental Prediction's (NCEP) Nested Grid Model (NGM). The data was obtained from a standard data archive maintained by the National Oceanic and Space Administration's Air Resources Laboratory (NOAA-ARL). NOAA-ARL routinely archives this NGM data in a format that can be read by the HYSPLIT_4 Modeling System. The standard NGM model domain encompasses the contiguous United States and Canada with a latitudinal and longitudinal grid spacing of approximately 90 km. Due to storage space considerations, the NOAA-ARL's archived NGM data set contains information from only every other grid point in the domain and thus has a reduced resolution of approximately 180 km by 180 km. There are ten vertical levels in the model, stretching from the surface to 300 mb. At each gridpoint, data is available for the following variables: the U and V wind components, vertical velocity, temperature, specific humidity, and pressure. The data from the NOAA-ARL archive is available in two-hour intervals.

Previous research has suggested that the atmospheric deposition of mercury to South Florida is dominated by wet-deposition, with the majority of this deposition associated with summertime convective precipitation events (Dvonch *et al.* 1998;

Guentzel *et al*. 1995). The precipitation events typically occur during the mid- to late-afternoon hours in South Florida and thus daily back-trajectories were calculated for 2000 GMT each day.

b. Clustering of atmospheric transport back-trajectories

A number of previous studies have been conducted that employ objective analyses of meteorological flow regimes. Moody and Samson (1989) used a statistical technique to perform a cluster analysis of two-dimensional mixed layer back trajectories in an effort to determine what fraction of chemical variability in acidic precipitation composition could be related to differences in atmospheric transport. Their results suggested that from 10 to 40 percent of the precipitation chemistry variability could be accounted for by differences in atmospheric transport regimes. Similar objective statistical techniques linking atmospheric transport regimes with precipitation chemistry variability have been employed by Fernau and Samson (1990), Dorling *et al*. (1992 a, b), Dorling and Davies (1995) and Brook *et al*. (1995).

In short, cluster analysis is an objective mathematical technique whereby large datasets can be divided into similar groups or clusters that reflect some underlying structure that is within the dataset. The goal is to have within-cluster members differ from each other as little as possible, while having each cluster as distinct from the other clusters as is possible. For this analysis, the goal was to identify distinct meteorological flow regimes which would likely lead to distinct wet- and dry-deposition patterns. Weighting each cluster by its monthly and annual frequency of occurrence results in an estimate of the monthly and annual deposition without the necessity of modeling every day of the year-long period studied.

The daily 72-hour back-trajectory data was analyzed using the SAS statistical analysis package (SAS Institute, Cary, NC). The SAS CLUSTER procedure was used to hierarchically cluster the observations using the Ward's Minimum Variance Method. This method is based upon the idea that the greatest amount of information is available when a set of *n* members is ungrouped. Therefore, the grouping starts with *n* member acting as *n* separate groups. The initial step is to select two of these *n* separate groups which when united, will reduce the number of groups to *n*-1, while resulting in the least amount of lost information. If desired, the process may be continued until only one group, with *n* members, remains. Specific details on the method can be found in Ward (1963).

In its implementation of Ward's minimum variance method, the SAS CLUSTER procedure determines the distance between two clusters as the ANOVA sum of squares between the two clusters added up over all of the variables. In this study, the variables are the observed precipitation amount and trajectory end points, which correspond to air parcel locations at T_0 (trajectory end time, 20Z), T_0-1 hour, T_0-2 hours, etc. With each new generation (or iteration) of the analysis program, a squared multiple correlation coefficient, R^2, is calculated. In this case, R^2 represents that portion of the variance accounted for by the current number of clusters. By monitoring the decrease in R^2 following each iteration of the program, one can determine the degree of information loss that is acceptable, beyond which further clustering of the data does not provide useful information. During our analysis, a considerable degradation in the amount of variance explained by the remaining clusters became evident for generations in which the data set was grouped into fewer than eight clusters ($R^2 < 0.80$). For this reason, it was determined that the use of eight clusters would reduce the data set to a manageably low number of atmospheric transport regimes that could be modeled, without sacrificing a large amount of statistical information. Eder *et al*. (1994), among others, have suggested the use of Average Linkage Techniques in the objective clustering of meteorological data. Both the Ward's Minimum Variance Method and the Average Linkage Technique were tested for this study, with the Ward's Minimum Variance Method doing a superior job of producing clusters that could be attributed to distinct, meteorological atmospheric flow regimes. As such, the output from the Ward's Minimum Variance Method was used.

The original research plan had called for the clustering of the back-trajectories using the hourly endpoints for the entire 72-hour history of the air parcel back-trajectories. However, the proximity of South Florida to the southern boundary of the NGM domain resulted in the back-trajectories for a number of days originating from locations out of the NGM model boundary. As a result, the full 72-hour length of these back-trajectories could not be computed without a large number of missing end points. When using the SAS CLUSTER procedure, back-trajectories with missing data points are removed prior to clustering. After reviewing the back-trajectory database, it was felt that 12 hours of back-trajectory information would allow us to adequately characterize the atmospheric flow regime impacting South Florida on a given day while maximizing the number of clusters included in the objective clustering routine. The use of only 12 hours of back-trajectory data still resulted in approximately 60 days being removed from the clustering analysis due to missing data points. As a result, following the completion of the objective grouping of the back-trajectories, Daily Weather Maps from the National Oceanic and Atmospheric Administration (NOAA) were used to evaluate each day of the year-long period to determine if the clustering resulted in accurate meteorological clusters. This careful analysis of the daily maps provided independent validation of the trajectory clustering approach. Detailed analysis of the daily NOAA maps was then used to place the remaining days, those which had missing trajectory data, into the objectively obtained clusters.

c. Mesoscale modeling of representative cluster days

Following the determination of the dominant meteorological flow regimes impacting South Florida during our study period, the next step in our analysis was to model the three-dimensional meteorological fields across the area for use in the dispersion and deposition calculations. Two representative days from each of the obtained clusters where chosen for modeling. Where possible, these days were chosen such that they represented extremes in the spatial nature of the atmospheric transport and deposition for the given cluster. It was hoped that in doing so, this would minimize potential biases that could possibly be introduced by choosing two days with nearly identical deposition patterns. The days chosen for modeling are presented in Table 1 below:

TABLE 1

Representative Cluster Days Chosen for Hybrid Modeling Exercise

Cluster Number	Wet Days	Dry Days
1	29 MAY 1996 09 SEP 1995	22 FEB 1996 27 JUN 1995
2	13 MAY 1996 16 AUG 1995	20 SEP 1995 06 JUN 1996
3	11 SEP 1995 13 JUN 1996	17 DEC 1995 30 MAR 1996
4	11 MAR 1996 29 SEP 1995	23 OCT 1995 07 FEB 1996
5	19 MAR 1996 09 APR 1996	17 FEB 1996 21 MAR 1996
6	23 JUN 1996 27 MAY 1996	13 APR 1996 07 MAR 1996
7	02 MAR 1996 15 OCT 1995	12 JAN 1996 22 MAY 1996
8	Not Modeled	03 MAR 1996 23 DEC 1995

Due to the geographical characteristics of South Florida, the transport, dispersion and deposition (both wet and dry) of pollutants across this region are controlled by circulation patterns that range from the meso- to synoptic-meteorological scales. For this reason, the modeling efforts associated with this project required the use of a mesoscale meteorological model to accurately describe the three-dimensional meteorological fields across South Florida during the study period. The Regional Atmospheric Modeling System (RAMS) (Pielke *et al*. 1983) was selected for use in our study, given its previous successful use in investigations involving lake-/sea-breeze circulations for a number of coastal areas across the United States. As an example, Eastman and Pielke (1995) used RAMS to study lake breeze circulations by comparing RAMS model output with tracer data. Lyons *et al*. (1995 a) used RAMS to provide input to a photochemical model for the Lake Michigan Ozone Study (LMOS). Lyons *et al*. (1995 b) also used RAMS to investigate wind flow/sea breeze regimes across Florida.

The present study took advantage of the nested grid-structure capability that is available in RAMS. The first grid encompassed the eastern United States, with a mesh size of 60 km using 50 x 50 horizontal grid points. The second grid (nested within Grid One) encompassed the southeastern U.S. with a mesh size of 20 km using a 62 x 62 horizontal grid points. The third grid (nested within Grids One and Two) encompassed South Florida, with a mesh size of 5 km using a 50 x 50 horizontal grid points. All three grids used 34 levels in the vertical with a vertical grid spacing of 50 m near the surface, with vertical grid spacing stretching to 850 m near the model top at approximately 15 km. The meteorological fields resulting from the RAMS model simulations (for Grids Two and Three) were saved every hour for the duration of the simulation for use as input for the wet- and dry-deposition calculations using the HYSPLIT_4 Modeling System (Draxler and Hess,1997) during the next stage of the analysis.

The RAMS model was initilized with meteorological fields derived from the NCEP's NGM. Given that the mesoscale convective features that play an important role in mercury wet-deposition in South Florida can extend beyond the 300mb, the NGM data fields archived by the NOAA-ARL could not be used, since this data does not extend beyond the 300mb vertical level. As a result, NGM data fields archived by the University of Michigan were used to initialize the RAMS model. The data fields archived by the University of Michigan had a horizontal resolution of 250 km (E-W) by 125 km (N-S) with a vertical extension to 100 mb.

Given the importance of land-ocean temperature differences in controlling the occurrence and magnitude of land/sea-breeze circulations, weekly average sea-surface temperature data was obtained from NCEP to be used as input fields for the RAMS simulations. This data is satellite derived and has a global 1° by 1° resolution.

d. Dispersion and deposition modeling

The dispersion and depositional modeling portion of this project used the HYSPLIT_4 Modeling System (Draxler and Hess, 1997). As noted earlier, HYSPLIT_4 is a complete modeling system that can be used for a range of meteorological/air quality applications ranging from the calculations of simple forward- and/or backward-trajectories to the performance of complex dispersion/deposition simulations. For this portion of our study, HYSPLIT_4 was executed using the medium resolution (20 km x 20 km) meteorological output fields from the RAMS simulations discussed in the previous section (Grid Two). The model allows the user to specify the number of emissions sources to be studied, the location of each source in the x, y and z directions, the emission rate and duration of emission. HYSPLIT_4 can treat both particles and gaseous pollutants for either continuous or puff releases, with the model simulations presented in this paper using the continuous release option.

The emissions database used for this work is the same as that used for the RELMAP (Bullock *et al*., 1997) mercury modeling simulations performed for, and discussed in, the United States Environmental Protection Agency (US EPA) Mercury Study Report to Congress (US EPA 1997). The US EPA mercury emissions database includes speciated information for both area- and point-source emissions, with a summary of the standard speciation profiles used for point-source emissions listed in

TABLE 2. A complete listing of the point sources used in this study can be found in TABLE C1 of Appendix C. The US EPA mercury emissions database considered area source emissions to be only in the elemental form, Hg(0), and accounted for only 2 percent of the total emissions. As a result, area sources were not considered in this work.

TABLE 2
Mercury Emissions Inventory Used In Current Study

Mercury Emission Source Type	**Speciation Percentages**		
	Hg(0)	**Hg(II)**	**Hg(p)**
Municipal Waste Combustion	20	60	20
Medical Waste Incinerators	2	73	25
Electric Utility Boilers (coal, oil, gas)	50	30	20
Commercial and Industrial Boilers	50	30	20
Hazardous Waste Incinerators	As specified per location in EPA database		

Once released, particulate and vapor phase pollutant transport, dispersion and deposition are explicitly calculated. HYSPLIT_4 has three different pollutant removal mechanisms: dry-deposition, wet-deposition and radioactive decay (not relevant to this work). For the simulations presented in this report, dry-deposition processes were addressed by explicitly defining both particle and vapor phase dry-deposition velocities. The deposition values used, for daytime and nighttime periods respectively, were set at 0.025 and 0.013 cm/s for Hg(0), 2.50 and 1.25 cm/s for Hg(II) and 0.45 and 0.23 cm/sec for Hg(p).

The daytime deposition velocities noted above were based upon those suggested by Shannon and Voldner (1995). However, the nighttime deposition values suggested by Shannon and Voldner (1995) were lower than those measured by the University of Michigan Air Quality Laboratory during the 1999 Florida Everglades Dry Deposition

Study (FEDDS). During the 1999 FEDDS, surrogate surface measurements of total mercury dry-deposition were made during the two-week study period, as were ambient measurements of particulate and vapor phase mercury. These data were used to obtain estimates of nighttime deposition velocities for Hg(II). These results suggested that the nighttime deposition velocities were, on average, approximately one-half of the daytime velocities. As a result, this study assumed that the nighttime deposition velocities for all species were one-half of their daytime values. For our modeling study, the daytime period corresponded to 0900 to 1600 LT.

Within HYSPLIT_4, the wet-deposition follows that of Hicks (1986) and is divided into two distinct processes: those in which the pollutants are continually ingested into a cloud from the polluted boundary layer (within cloud scavenging) and those in which rain falls through the polluted boundary layer (below cloud scavenging). Gaseous wet-removal of Hg(0) and Hg(II) was considered by specifying the Henry's Law constants for each species: 0.112 M atm^{-1} and 2.1×10^3 M atm^{-1}, respectively. The value typically assumed for Hg(II) is that used for HNO_3: 2.1×10^5 M atm^{-1}. However, use of this value resulted in unrealistically high values of mercury wet-deposition to the Davie site when compared with our observed event-precipitation data set. Improved agreement was found using the lower value and thus this value was used for the modeling study. Interestingly, the lower Henry's Law constants used did not significantly effect the average deposition to South Florida or to WCA3, and only effected the grid squares in which the major sources were located. Finally, the particle wet removal coefficients for both within- and below-cloud removal processes were also explicitly set, using values suggest by Draxler and Hess (1997).

TABLE 3. Summary of "clustered" atmospheric transport regimes and precipitation statistics associated with each cluster based upon data collected at Davie, Florida during the 1995-96 SoFAMMS study period.

Cluster Number	Description of flow regime represented	No. of Days within cluster	No. of Days with Rainfall (Davie, FL)	Total Rainfall for Cluster (cm) (Davie, FL)	Volume Weighted Mean Concentration for Cluster (ng/L) (Davie, FL)	Total Hg Wet-deposition observed ($\mu g/m^2$) (Davie, FL)
1	Weak local flow, variable in direction	65	18	12.1	31.8	3.84
2	Weak synoptic flow from north	35	5	2.7	29.2	0.79
3	Moderate local/synoptic flow from east	104	30	26.2	20.9	5.47
4	Strong synoptic flow from northeast.	48	8	22.1	10.8	2.39
5	Strong synoptic flow from northwest	32	9	6.9	10.6	0.73
6	Moderate synoptic flow from south	58	29	94.0	14.5	13.64
7	Moderate synoptic flow from southwest	11	4	8.7	12.8	1.12
8	Strong synoptic flow from north	13	1	0.1	7.1	0.01

3. Cluster analysis results

As noted previously, eight different atmospheric transport clusters were obtained through the cluster analysis procedure. Given that the distributions of total mercury wet-deposition for each cluster exhibited departures from normality, and given the unbalanced nature of the clusters due to their small size in terms of the number of wet-deposition events per cluster, it was necessary to use a non-parametric test for statistical comparisons between clusters. In the work by Moody and Samson (1989), significant differences among transport groups could be reported when the null hypothesis of no difference in distributions could be rejected at the 95 percent confidence level using the Kruskal-Wallace test, a non-parametric one-way analysis of variance test. Using this test and the clusters obtained during our analysis, the null hypothesis of no differences in distributions was rejected at the 95 percent confidence level.

A summary of the eight atmospheric transport clusters obtained in this analysis is presented in Table 3. The general nature of these clustered back-trajectory groups are described below, with plots of each cluster found in Appendix A. Maps of the surface meteorological features for days representative of each cluster can be found in Appendix B.

The first cluster identified by this analysis is presented in Figure A1 and can best be described as characterizing days with weak, local flow. An analysis of daily surface weather maps indicated that the flow regimes included in this cluster were generally associated with weak centers of high pressure centered over South Florida. The second cluster identified is presented in Figure A2. This cluster is again characterized by weak flow, but of a synoptic influence. Days included within Cluster 2 generally were influenced by both weak high and low-pressure systems over and near the Florida peninsula. Stronger flow is evident for those days included as part of Cluster 3 (Figure A3). The days included in this cluster were characterized as having moderate flow from the east, typically associated with varying extents of influence from the semi-permanent Bermuda High. Initially, attempts were made to separate the easterly flow into those days with easterly synoptic flow and those days with mainly locally produced sea-breeze circulations. However, it was found to be very difficult to separate a purely “sea-breeze” day (when no significant synoptic forcing was present) from those days when the sea-breeze forcings were superimposed over weak easterly synoptic flow. As a result, no separation was performed for this analysis.

Cluster 4 (Figure A4) is characterized by strong synoptic flow, northeasterly in direction, which was generally associated with strong high-pressure centers over the East Coast of the United States. Days included in this cluster category often followed days that had experienced a cold frontal passage across South Florida. Strong synoptic flow was also a characteristic of those days included in Cluster 5 (Figure A5). These days were characterized as having strong northwesterly flow, generally associated with the advance of a strong Southern Plains high-pressure area following a cold frontal passage across South Florida. Clusters 6 (Figure A6) and 7 (Figure A7) were also associated with flow patterns influenced by passing cold frontal boundaries. The days in Cluster 6 were characterized by southerly flow, typically in advance of cold frontal boundaries. Cluster 7 days were those that were influenced either by nearly stationary cold frontal boundaries, weak residual troughs or multiple frontal boundaries positioned across South

Florida so as to result in southwesterly flow. Finally, Cluster 8 (Figure A8) was characterized by moderate to strong synoptic flow from the north, generally associated with advancing areas of high-pressure in the Central and Southern Plains.

As seen in Table 3, the clusters with the highest observed volume-weighted mean Hg concentrations were Clusters 1-3, despite the fact that these clusters experienced some of the largest rainfall totals. However, these clusters were characterized by weak to moderate atmospheric transport patterns. These weaker flow regimes likely resulted in relatively low boundary-layer ventilation rates (the product of the horizontal wind speed and the boundary layer height) compared to the other cluster categories. Such conditions would be consistent with a relatively higher pollutant burden from local sources remaining in South Florida, resulting in a relatively higher concentration of pollutants (including Hg) in rainfall. The data presented in Table 3 also indicates that elevated volume-weighted mean Hg concentrations alone did not explain the observed total Hg wet-deposition at the Davie, FL site on a cluster-by-cluster basis. Despite having relatively low volume-weighted mean Hg concentrations, Clusters 4 and 6 reported relatively high total Hg wet-deposition fluxes, likely due to relatively high amounts of observed precipitation.

4. Modeling Study Results

a. Model Sensitivity Analysis

The hybrid-model estimates of speciated mercury wet- and dry-deposition are sensitive to a number of input parameters. The three major factors include: meteorological fields, emissions estimates (mass rate and speciation) and other user specified input parameters (such as Henry's Law coefficient for reactive gaseous mercury). In this section, we shall discuss a number of analyses that were made in order to better understand the impact associated with changes and/or variations in these factors.

Sensitivity of Total Mercury Deposition to Meteorological Variability

Given the spatial complexity of the meteorological fields employed in this modeling effort, a global sensitivity analysis of the hybrid model's wet- and dry-deposition estimates to all emissions and meteorological parameters is beyond the scope of this study. However, it is important to provide some illustration of the variability of the hybrid model's wet- and dry-deposition estimates as a function of varying meteorology. For this purpose, Figures 2 and 3 present the modeled 24-hour total mercury dry- and wet-deposition estimates for SFWMD WCA3 as a function of atmospheric transport cluster category. The 24-hour deposition estimates for each day listed in Table 1 are presented in an effort to show the within-cluster variability, as well as the between-cluster variability. It should be remembered that in an effort to avoid biasing model results toward a given flow pattern, the days chosen to represent a given cluster were chosen to represent spatial extremes in the deposition pattern associated with that cluster. It was felt that this would result in a more robust average deposition and a conservative standard deviation for a given cluster.

Inspection of Figure 2 indicates that there is considerable variability in the modeled 24-hour dry-deposition to SFWMD WCA3 as a function of atmospheric transport cluster. Some clusters, such as Clusters 5 and 7, show little deposition to SFWMD WCA3 given that most of the local source emissions are transported away from the site. In contrast, Clusters 2-4 and 6 showed the potential for relatively greater dry-deposition due to the onshore nature of the flow. The degree of within-cluster variability differed as a function of cluster, as well. For Clusters 1,5 and 7 (for which one would expect less impact from local sources), there was good agreement between Day 1 and Day 2 estimates, suggesting relatively little variability on a day to day basis under these flow conditions. One could infer that less accurate wind input data for these three clusters would not likely contribute significantly to deposition uncertainties in the model estimates, since variations in atmospheric transport within these cluster groups do not result in much variation in deposition estimates. For Clusters 2, 3 and 4 (for which one would expect greater impact from local point sources), there was relatively large differences between Day 1 and Day 2 estimates. These relatively large within-cluster differences suggest that small changes in flow can greatly effect the extent to which SFWMD WCA3 is impacted by a specific source(s). For this reason one could infer that less accurate wind input data for these three clusters could contribute significantly to deposition uncertainty in the model estimates, since variations in atmospheric transport within these cluster groups result in significant variation in deposition estimates. It is precisely for this reason that a significant effort was expended in defining the local wind flows using RAMS as described earlier.

A comparison of the variability in model estimates of the 24-hour wet-deposition of total mercury to the SFWMD WCA3 is presented in Figure 3. As was true for dry-deposition (discussed above), model results suggest that there is considerable between-cluster, as well as within-cluster, variability. For Clusters 5 and 7, the wet-deposition estimates for both days are quite similar, albeit low. Again, these two clusters represent atmospheric transport regimes that consist of offshore flow (taking local emissions away from SFWMD WCA3) and thus variability in the specified wind direction/transport have little impact on wet-deposition to WCA3. For clusters with predominant onshore transport, significant within-cluster can again be seen. This suggests that for these clusters, relatively small changes in the predominant flow can lead to noticeable differences in wet-deposition to SFMWD WCA3. For this reason, a lack of precision in estimates of wind direction and wind speed could lead to relatively larger errors in estimated wet-deposition to a specific location such as WCA3.

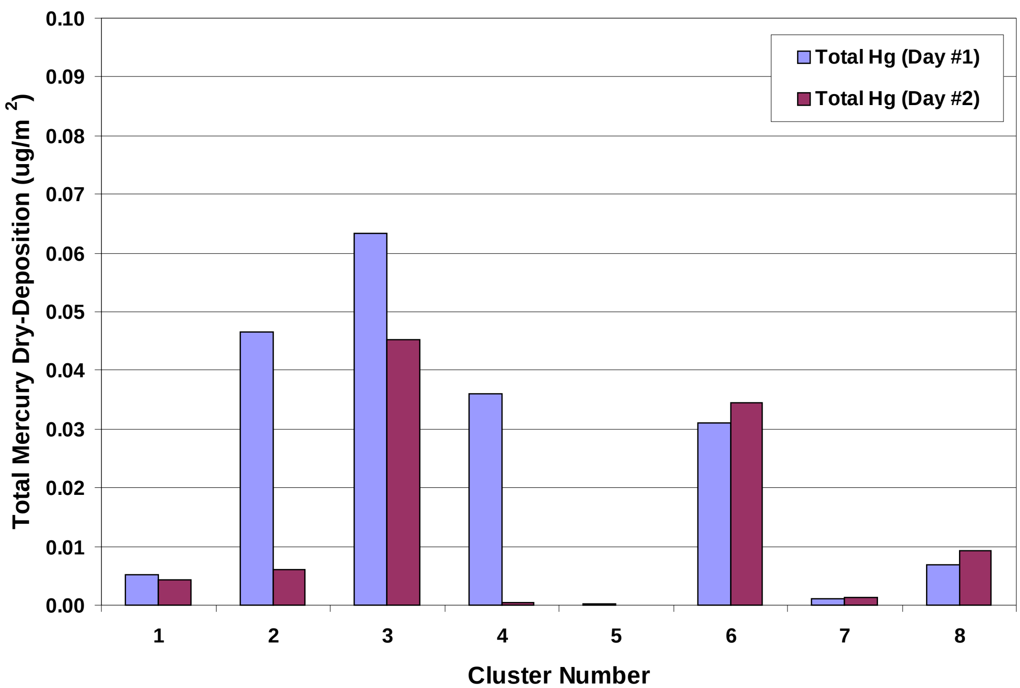

Figure 2. Comparison of modeled 24-hour dry-deposition to SFWMD WCA3 as a function of atmospheric transport cluster (and day within cluster).

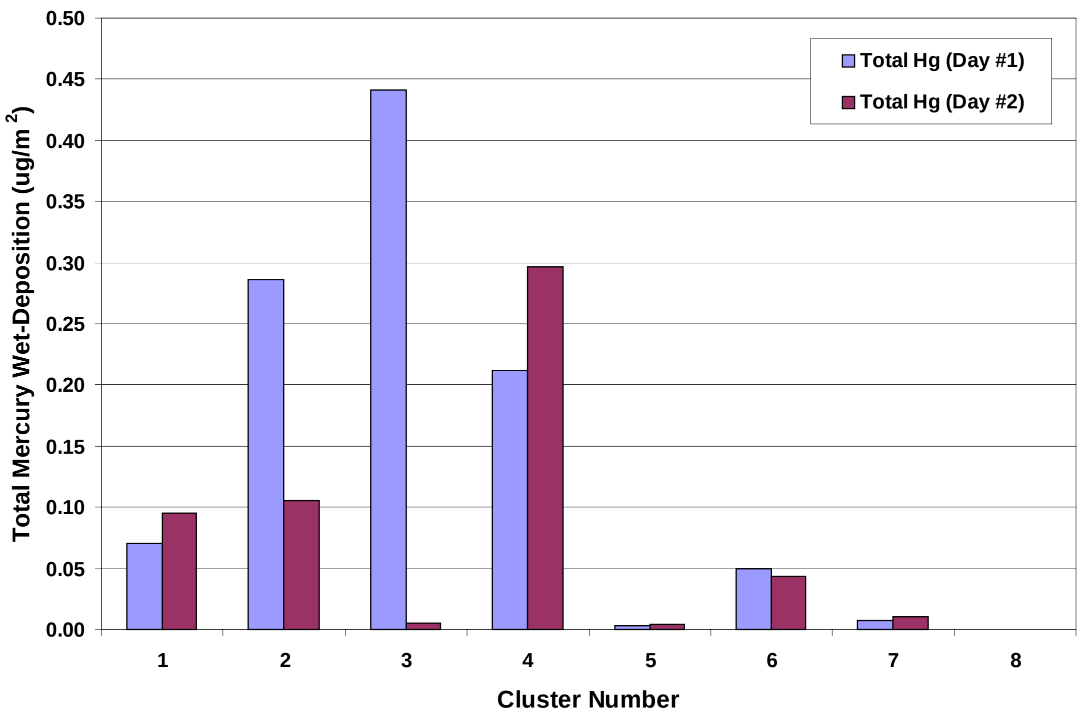

Figure 3. Comparison of the modeled 24-hour wet-deposition to SFWMD WCA3 as a function of atmospheric transport cluster (and day within cluster).

Sensitivity of Total Mercury Deposition Due to Emissions Variability

As one might expect, the estimates of total mercury wet- and dry-depositional loading to the SFWMD WCA3 are highly sensitive to the magnitudes of emissions used in our simulations, as well as to the relative *speciation* of mercury [Hg(0), Hg(II) and Hg(p)] used for simulations. In this section, we present findings regarding the sensitivity of the total mercury deposition estimates to changes in both of these factors.

Comparison of Different Total Mercury Emission Rates

Figure 4 presents the estimates of the total mercury dry-deposition to SFWMD WCA3 for the three emissions scenarios presented in this work [detailed in Section 4c]. Scenario #1 represents our BASE CASE, where the emissions were specified using those employed in the 1997 USEPA Mercury Report to Congress. In Scenario #2, the emissions database was modified using the stack testing results reported in Dvonch *et al.* (1999), namely changing the emission rates of two Dade County mercury sources where actual stack tests were performed. Specifically, the total mercury emissions from a Dade County medical waste incineration facility (MedX, Inc.) was changed from 9.2 kg/year to 100.4 kg/year and the total mercury emissions from the Dade County Resource Recovery Facility (municipal waste incinerator) was changed from 1,156.1 kg/year to 255.0 kg/year. For Scenario #3, the changes made in Scenario #2 were applied to all medical and municipal waste incineration sources in the modeling domain.

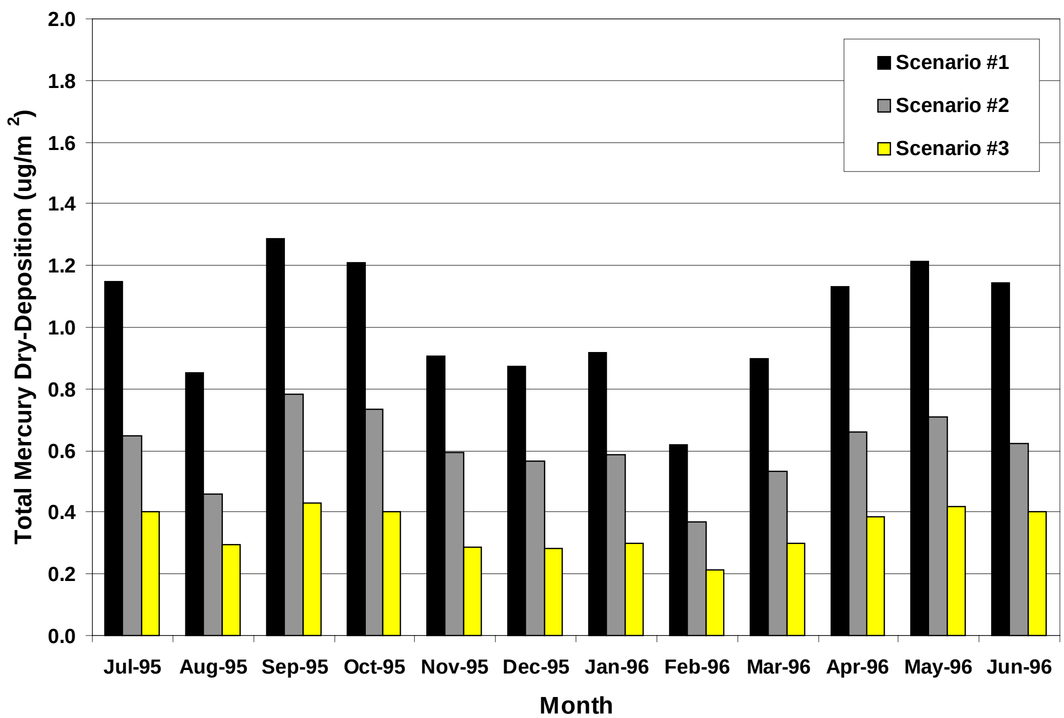

Figure 4. Comparison of the modeled monthly dry-deposition to SFWMD WCA3 as a function of emissions scenario.

Inspection of Figure 4 shows that significant differences are apparent for the monthly total mercury dry-deposition to WCA3 for the three scenarios used in this work.

In terms of annual differences, the estimated annual dry-depositional loadings of total mercury to WCA3 for Scenarios 1-3 are 12.2, 7.3 and 4.1 $\mu g/m^2$/year, respectively. These results suggest that uncertainties in the actual mass emissions of mercury from two of the largest point sources (Scenario #2) can have a pronounced impact on the modeled estimates of the total mercury dry-depositional loading to WCA3.

Similarly, pronounced differences between the three emission scenarios can be seen in the modeled estimates of the total mercury wet-depositional loading to WCA3, presented in Figure 5. The estimated annual wet-depositional loadings of total mercury to WCA3 for Scenarios 1-3 are 18.7, 10.3 and 7.1 $\mu g/m^2$/year, respectively.

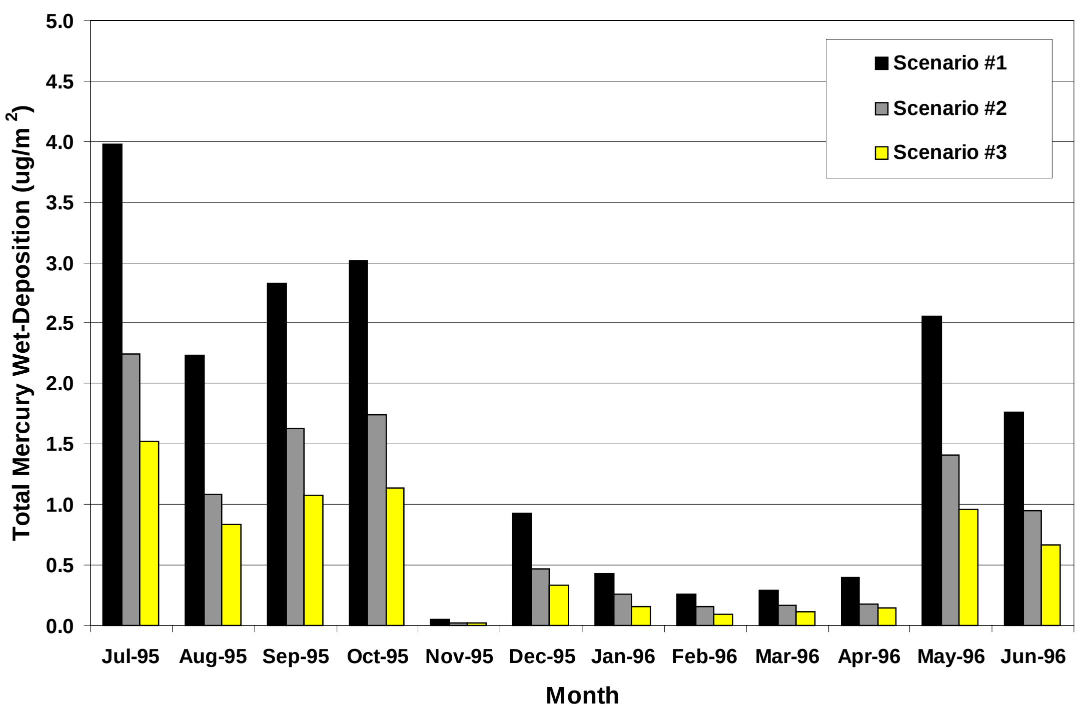

Figure 5. Comparison of the modeled monthly wet-deposition to SFWMD WCA3 as a function of emissions scenario.

Sensitivity of Estimates to Emissions Mercury Speciation

Given that each mercury species has unique characteristics (in terms of dry-deposition velocities and solubility in water), variations in the fraction of each species in the effluent from the different mercury sources may affect both the wet- and dry-depositional loading to WCA3. To simplify the sensitivity analysis, we modeled only those days associated with Cluster #3, the cluster that impacted WCA3 greatest. The first speciation used was taken from the 1997 US EPA Mercury Report to Congress (shown in Table 2). The second profile used was a slight modificiation (and is thus referred to as the modified profile) also uses the profile listed in Table 2, with two exceptions: medical waste sources where characterized as having 98 percent Hg (II) and 2 percent Hg (0) and municipal waste sources were characterized as having 80 percent Hg (II) and 20 percent Hg (0). The results of this comparison are shown in the Figure #6.

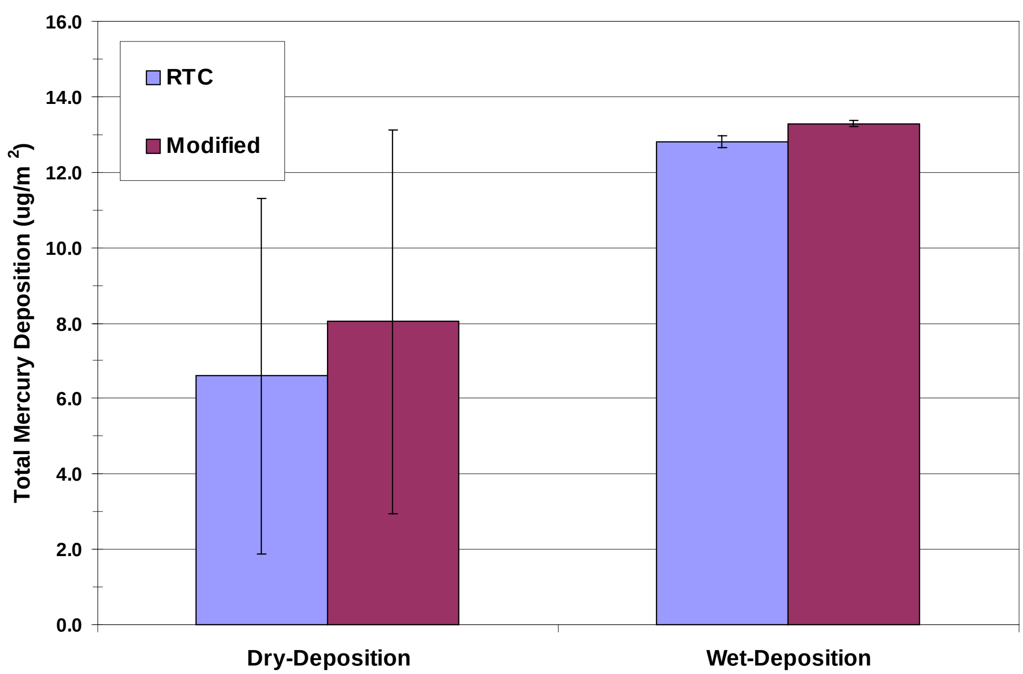

Figure 6. Comparison of the modeled total mercury deposition to SFWMD WCA3 for days within Cluster #3, using two different mercury speciation profiles.

Inspection of Figure 6 reveals that for both dry- and wet-deposition to WCA3, the modified speciation profile resulted in an increase in the total mercury loading to WCA3. For total mercury dry-deposition, estimates using the modified speciation profile resulted in an increase from $6.6 \pm 4.7\ \mu g/m^2$ to $8.0 \pm 5.8\ \mu g/m^2$, an increase of roughly 22 percent. For total mercury wet-deposition, estimates using the modified speciation profile resulted in an increase from $12.8 \pm 0.2\ \mu g/m^2$ to $13.3 \pm 0.1\ \mu g/m^2$, an increase of roughly 4 percent. The relative impact, at any given site, in the changes in emissions speciation will likely depend on the site location relative to major sources and source types. However, these results (particularly those of dry-deposition) suggest that the uncertainties in the Hg emission speciation from different source types is likely an important source of uncertainty in this and all future modeling efforts. As such, the development of improved speciation profiles for relevant mercury point source-types should be a major research priority.

Sensitivity of Total Mercury Deposition to Model Parameterizations

The HYSPLIT_4 model used in the estimation of both wet- and dry-deposition of mercury to SFWMD WCA3 allows for the specification of a number of parameters influencing the rates of dry- and wet-removal of mercury from the atmosphere. In this section, we present results of tests looking into the sensitivity of our results to changes in these removal rates.

Comparison of Different Mercury Dry-Deposition Velocities

As noted in Section 2d of this document, daytime deposition velocities for the three modeled species of mercury were set to those suggested by Shannon and Voldner (1995). The nighttime deposition velocities suggested by Shannon and Voldner (1995) were considerable lower than those observed during the 1999 FEDDS intensive, leading us to set nighttime deposition velocities to one-half of the specified daytime values (resulting in nighttime deposition velocities that were more in line with those obtained during the 1999 FEDDS intensive). The results presented in Figure 7 show the differences in the modeled total mercury dry-deposition to WCA3 for the case using solely the Shannon and Voldner (1995) specified dry-depositions and for the case in which the nighttime dry-deposition velocities were set to one-half of their respective daytime values (denoted as “This Study”). Figure 7 indicates that the use of the Shannon and Voldner (1995) dry-deposition velocities results in total mercury dry-deposition estimates that are considerabley lower than those using nighttime values of one-half daytime values. Annualized, the former results in a total mercury dry-deposition to WCA3 of 7.6 $\mu g/m^2$, while the latter results in an annual total mercury dry-deposition to WCA3 of 12.2 $\mu g/m^2$. These results suggest that present uncertainties in the dry-deposition velocities associated with the different species of mercury [particularly Hg (II)] can have a significant impact on modeled dry-deposition loading estimates. More research is needed to narrow the uncertainties in these dry-deposition velocities.

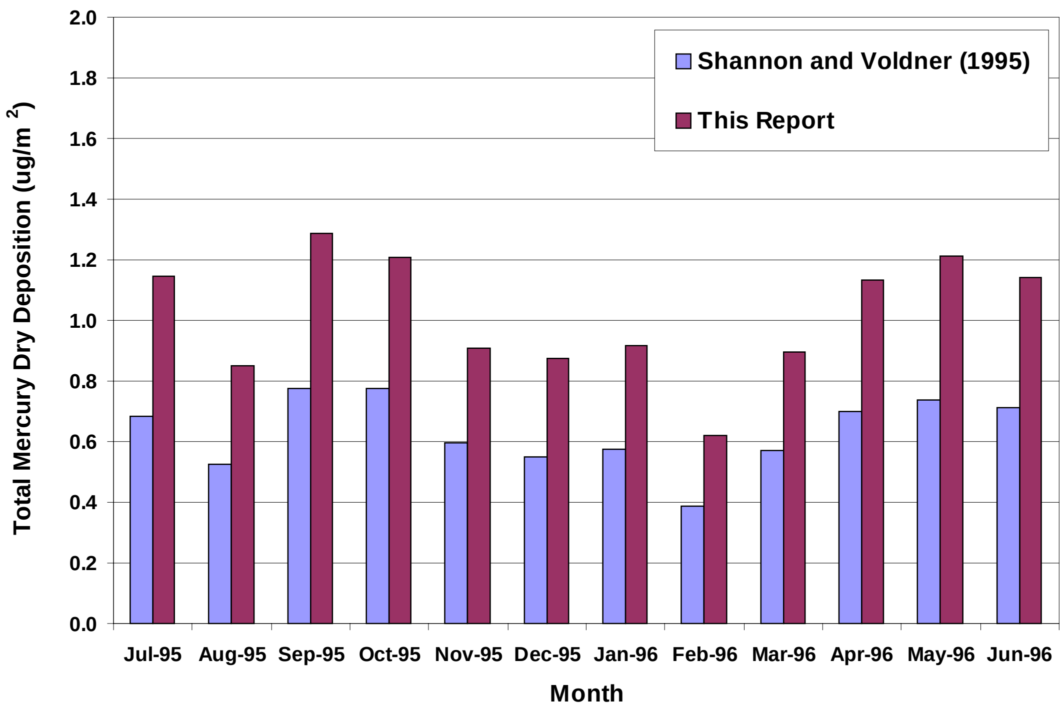

Figure 7. Comparison of the modeled monthly dry-deposition to SFWMD WCA3 using two sets of speciated dry-deposition velocities.

Comparison of Different Wet-Removal Rates

HYSPLIT_4's represents the wet-removal of gaseous mercury from the atmosphere as being proportional to the product of precipitation rate and the species dependent Henry's Law Coefficient. As noted in Section 2d above, the typical Henry's Law Coefficients used for the wet-removal of Hg(0) and Hg(II) are: 0.112 M atm^{-1} and 2.1 x 10^5 M atm^{-1}, respectively. These values are used by the HYSPLIT_4 model in the calculation of a below-cloud and within-cloud wet-removal rates for Hg(0) and Hg(II). A comparison of the modeled total mercury wet-deposition to SFWMD WCA3 and FAMS results for nearby stations (Tamiami Trail and Andytown) indicated that the modeled wet-deposition estimates were unreasonably high. In order to achieve better agreement between modeled and measured results, the wet removal rate for Hg(II) [the dominant form removed via wet-deposition processes] was reduced by introducing a factor of 10^{-2}. This reduction in the wet-removal rate for Hg(II) resulted in model wet-deposition estimates that were more in line with the observed FAMS data. Figure 8 shows a comparison of the modeled monthly total mercury wet-deposition for the SFWMD WCA3 using both the standard and reduced Hg(II) removal rates. In this case, the model results suggest that decreasing the removal rates used for Hg(II) resulted in an increase in the amount of total mercury wet-deposited to SFWMD WCA3. This increase is due to a reduction in the amount of Hg(II) that is removed by wet-removal processes closer to the sources, thus allowing more Hg(II) to be available for wet removal at SFWMD WCA3 and other downwind locations.

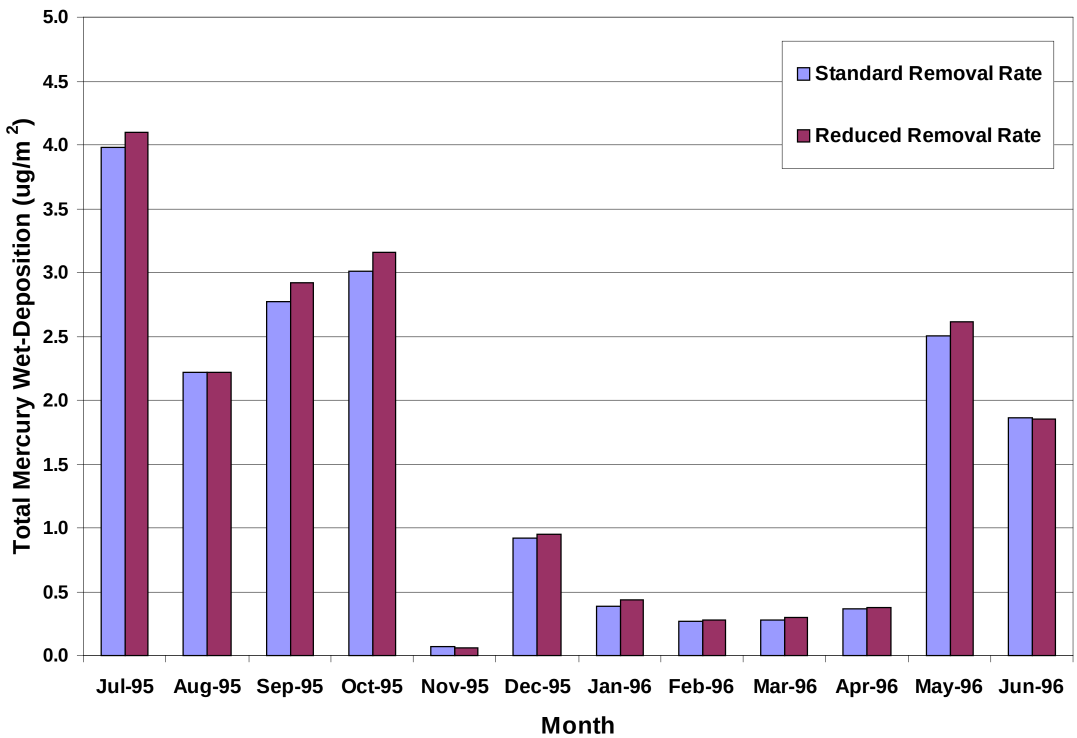

Figure 8. Comparison of modeled monthly total mercury wet-deposition to SFWMD WCA3 using two different values for the Hg(II) wet removal rate.

b. Model Validation Results

Calculation of Monthly Averages and Uncertainties

The model estimates of the monthly total mercury wet-deposition to the SFWMD WCA3 were computed as follows. First, the cluster average total mercury wet-deposition was computed using the following relationship:

$$\overline{Hg}_j = \frac{Hg_{j,Day1} + Hg_{j,Day2}}{2} \quad (1)$$

where $Hg_{j,Day1}$ and $Hg_{j,Day2}$ represent the modeled total mercury wet-deposition at the SFWMD WCA3 for the two representative days that were modeled for a given cluster, j. Monthly total mercury wet-deposition estimates for the site were then obtained by multiplying the average total mercury wet-deposition for a given cluster, j, by the number of occurrences of that cluster during the k^{th} month, then summing over all clusters:

$$\left[\overline{Hg}\right]_k = \sum_{j=1}^{8} \overline{Hg}_j \bullet n_j \quad (2)$$

Finally, an attempt was made to provide some measure as to the uncertainty in the model estimates of monthly total mercury wet-deposition. This was obtained by first computing the standard deviation of the wet-deposition estimates for each cluster. While it is fully understood that one does not typically calculate a standard deviation based upon two numbers, since the two days were chosen to represent the extremes for each cluster, the standard deviation does provide some measure of the variability in the model estimates for each cluster at the site. The weighted monthly uncertainty for the and month was computed as:

$$\sigma_k = \frac{\sum_{j=1}^{8} \sigma_j \bullet n_j}{\sum_{j=1}^{8} n_j}$$

where σ_j is the standard deviation in the cluster estimate of total mercury wet-deposition for cluster "j" at the site and n_j is the number of occurrences of cluster j events during the kth month.

Comparison of Model Estimates versus Observed Wet-Deposition Data

As an initial quality assurance check on the ability of our modeling approach to accurately estimate the monthly wet- and dry-deposition of mercury across South Florida, the model estimates of the monthly total Hg wet-deposition to the SFWMD WCA3 were compared with an average of the monthly observed total Hg wet-deposition to South Florida for the period studied, as represented by observations obtained from the Florida Atmospheric Mercury Study (FAMS) (provided by Curt Pollman, TetraTech). The FAMS sites used for this comparison were the Tamiami Trail Ranger Station and the Andytown site. These sites were selected for use in the validation exercise given that they border the SFWMD WCA3 to the south and north, respectively.

The comparison of the average observed monthly total mercury wet-deposition at the FAMS sites and the modeled total mercury wet-deposition to SFWMD WCA3 for the study period is presented in Figure 9. Overall, it can be seen that our hybrid modeling approach accurately portrays the very seasonal nature of the total mercury wet-deposition to South Florida. In terms of annual deposition, the modeled annual deposition of total mercury for the study period to the SFWMD WCA3 was 18.7 ± 6.2 μg/m^2, compared with an average for the two FAMS sites of 19.2 $\mu g/m^2$. On a monthly basis, it can be seen that the model and observed data compare less well during the months of July and August 1995. This disagreement is likely a result of the large uncertainty associated with Cluster #3 transport events (Figure 3), which occur with a relatively high frequency during these two months. However, during the remaining months of the year, the modeled and observed total mercury wet-deposition values compare quite well.

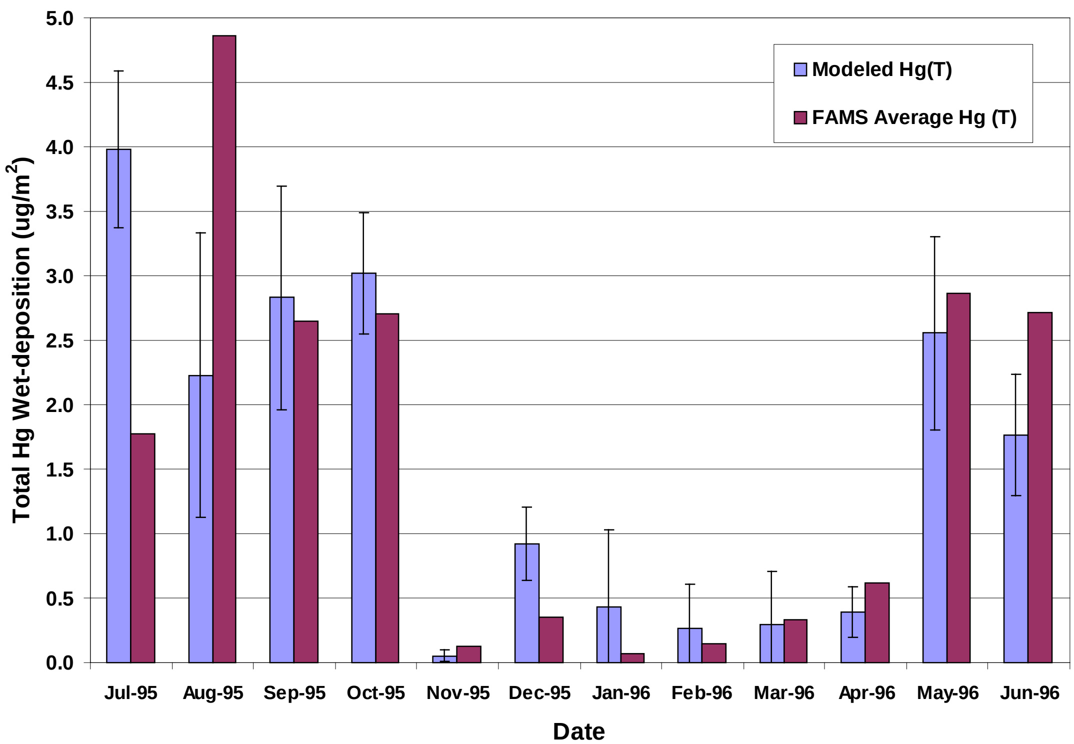

Figure 9. Comparison of the modeled monthly total mercury wet-deposition to SFWMD WCA3 for Scenario #1 and FAMS observed total mercury wet-deposition (average of Tamiami Trail Ranger Station and Andytown sites).

c. Hybrid Modeling Results

In this section, the final results are presented for the modeling runs performed as part of this project. Three different emissions scenarios were considered for both the wet- and dry-deposition modeling exercises. Model Scenario #1, our BASE CASE, employed the emissions inventory used for the RELMAP modeling exercises performed as part of US EPA's Mercury Study Report to Congress [USEPA RTC] (1977), which were based upon the estimated emissions for the year 1995. The USEPA RTC emissions inventory contained three mercury speciation categories (standard, 50% control and 85% control) for both *medical waste combustors* and *municipal waste combustors,* with each category have a separate relative speciation for mercury. The speciation percentages used in our Model Scenario #1 were those categorized by the USEPA RTC under the standard emissions control category. These speciation percentages were presented earlier in TABLE 2 of this document. The actual sources used during the modeling exercise are presented in Appendix C. Modeling Scenario #2 used the BASE CASE emissions inventory, with changes made to only two point-sources: a municipal waste incinerator (Dade County Resource Recovery Facility) and a medical waste incinerator (MedX, Inc., also in Dade County). The modified emissions of total mercury from these facilities were based upon stack testing conducted by the US EPA at these two facilities during the 1995 SoFAMMS (Stevens *et al*. 1996, in Dvonch *et al*. 1999). Based upon these stack test results, model Scenario #3 extended the modified emissions used in Scenario #2 to all of the municipal waste incinerators and medical waste incinerators within our modeling domain, as discussed in Dvonch *et al*. (1999). Specific results are presented below:

<u>Model Estimates of the Monthly Wet-deposition of Speciated Mercury to the SFWMD WCA3</u>

<u>Scenario #1: BASE CASE</u>

Scenario #1, our Base Case, incorporates the "standard" source specific mercury speciations used in the US EPA Mercury Study Report to Congress. These model results predict a total mercury wet-deposition of 18.74 ± 6.15 $\mu g/m^2$ to the SFWMD WCA3.

The temporal variation in the wet-deposition of total mercury to the SFWMD WCA3 is presented in Figure 10. Not surprising, the model estimates suggest a significant seasonal trend in total mercury wet-deposition to the area, predicting that over 80 percent of the wet-deposition should occur during the months of May through October.

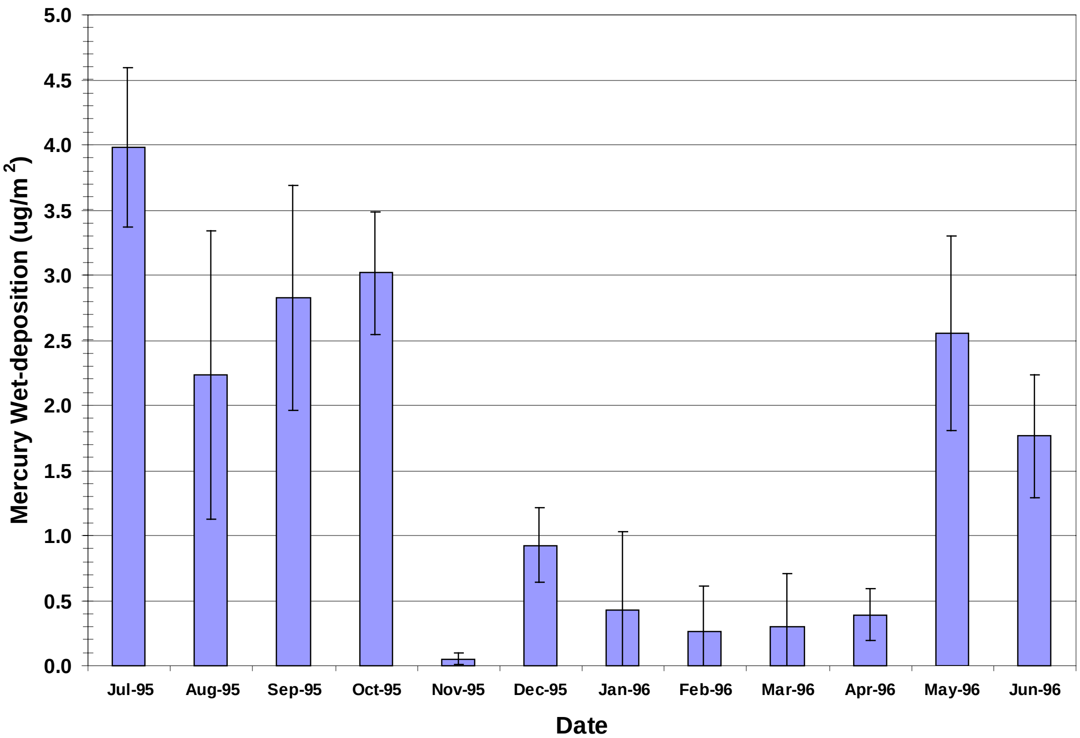

Figure 10. Modeled monthly Total mercury wet-deposition to SFWMD WCA3 for Scenario #1.

The speciated mercury wet-deposition is presented in Figure 11. From this figure, it can be seen that the total wet-deposition of mercury is predicted to be dominated by deposition of reactive gaseous mercury, believed to be in the form of Hg (II). In contrast, model results suggest that the deposition of gaseous elemental mercury, Hg(0), is relatively negligible. Once again, the seasonal nature of the deposition is apparent.

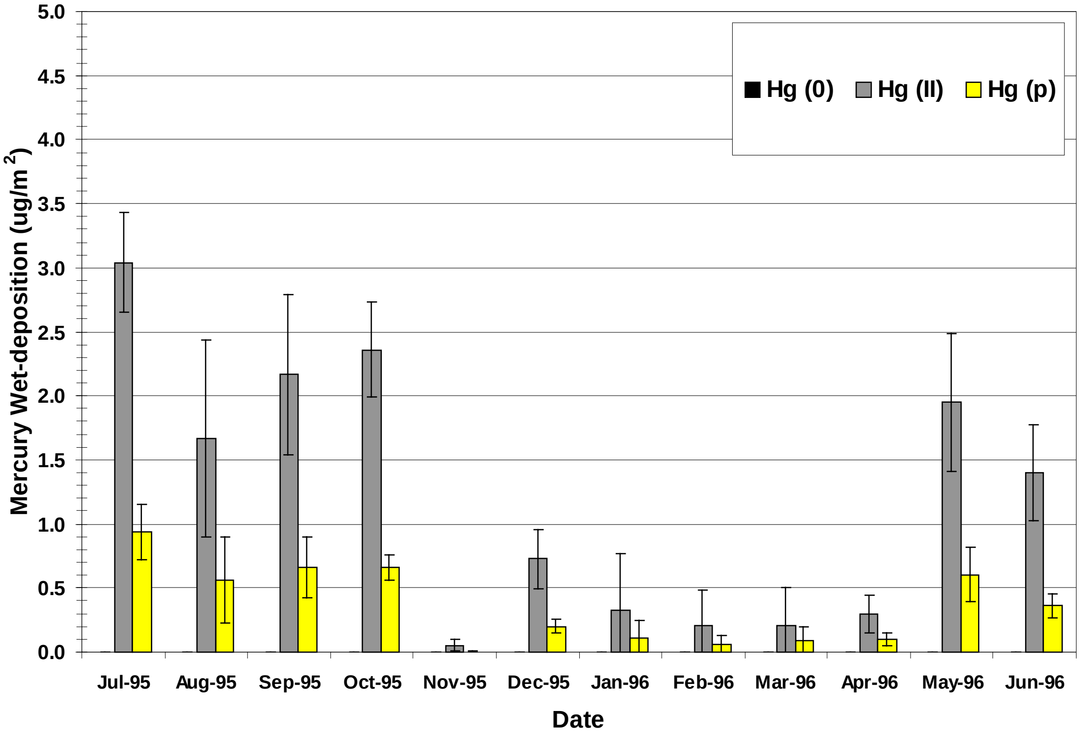

Figure 11. Modeled monthly speciated mercury wet-deposition to SFWMD WCA3 for Scenario #1.

Scenario #2

For Scenario #2, we used the emissions database employed in the US EPA Mercury Study Report to Congress, with modifications made to two specific point sources in Dade County: the Dade County Resource Recovery facility and the MedX, Inc medical waste incineration facility. These modifications resulted in the annual total mercury emissions from the Dade County Resource Recovery facility being changed from 1,156.1 kg/yr to 255.0 kg/year and the annual total mercury emissions from the MedX, Inc. facility being changed from 9.2 kg/year to 100.4 kg/year. The results of the modeled monthly total mercury wet-deposition for the Scenario #2 model run are presented in Figure 12.

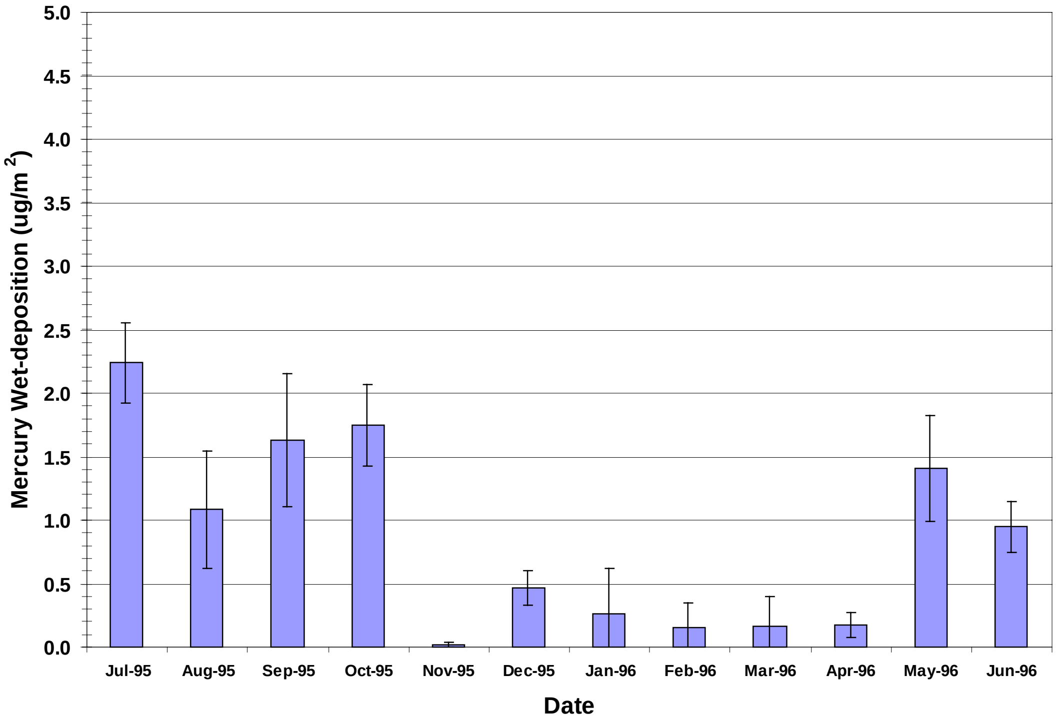

Figure 12. Modeled monthly total mercury wet-deposition to SFWMD WCA3 for Scenario #2.

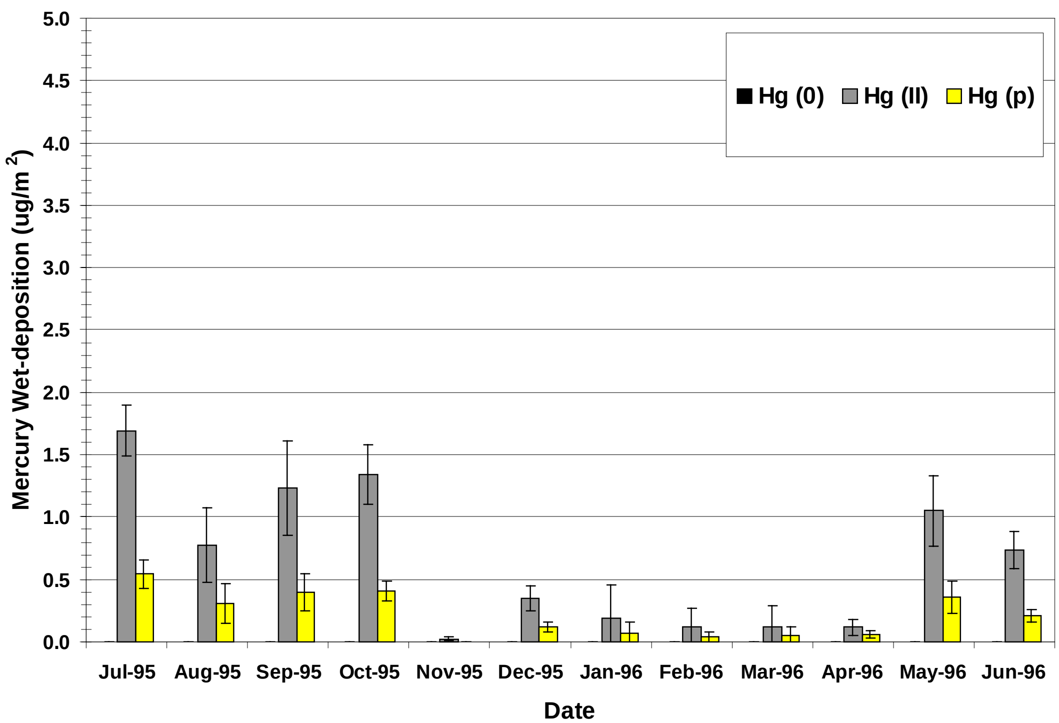

Figure 13. Modeled monthly speciated mercury wet-deposition to SFWMD WCA3 for Scenario #2.

The hybrid-modeling approach resulted in predicted total mercury wet-deposition to the SFWMD WCA of 10.31± 3.28 μg/m^2, roughly 55 percent of the predicted total mercury wet-deposition obtained in Scenario #1. Despite the reduction in the magnitude of the total mercury wet-deposition to SFWMD WCA3 for Scenario #2, the overall seasonal trend in total mercury wet-deposition is still evident.

The speciated mercury wet-deposition for Scenario #2 is presented in Figure 13. From this figure, it can be seen that the total wet-deposition of mercury is once again predicted to be dominated by deposition of reactive gaseous mercury, with a negligible contribution from elemental mercury.

Scenario #3

The modeled monthly total mercury wet-deposition to SFWMD WCA3 for Scenario #3 is presented in Figure 14. As might be expected from our Scenario #2 results, the Scenario #3 results indicated an reduction in the total annual wet-depositional loading to WCA3 for the period studied. The annual total mercury wet-deposition to WCA3 was estimated to be 7.1 ± 2.1 μg/m^2, a value that is approximately 38 percent of the Scenario #1 wet-deposition estimate.

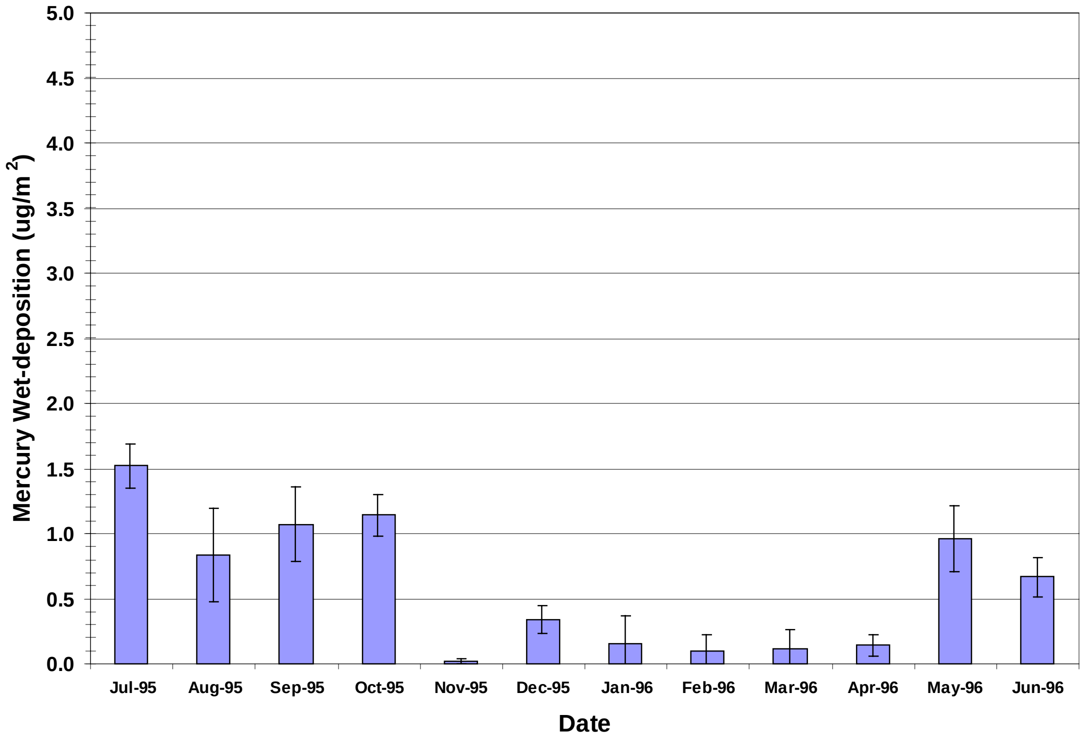

Figure 14. Modeled monthly total mercury wet-deposition to SFWMD WCA3 for Scenario #3.

The speciated mercury wet-deposition to WCA3 for Scenario #3 is presented in Figure 15. Like the first two modeled scenarios, the seasonality in the speciated wet-deposition is still evident and Hg(II) continues to be the dominant species deposited. The most significant change is, of course, that the absolute magnitudes of the wet-deposition fluxes are significantly reduced.

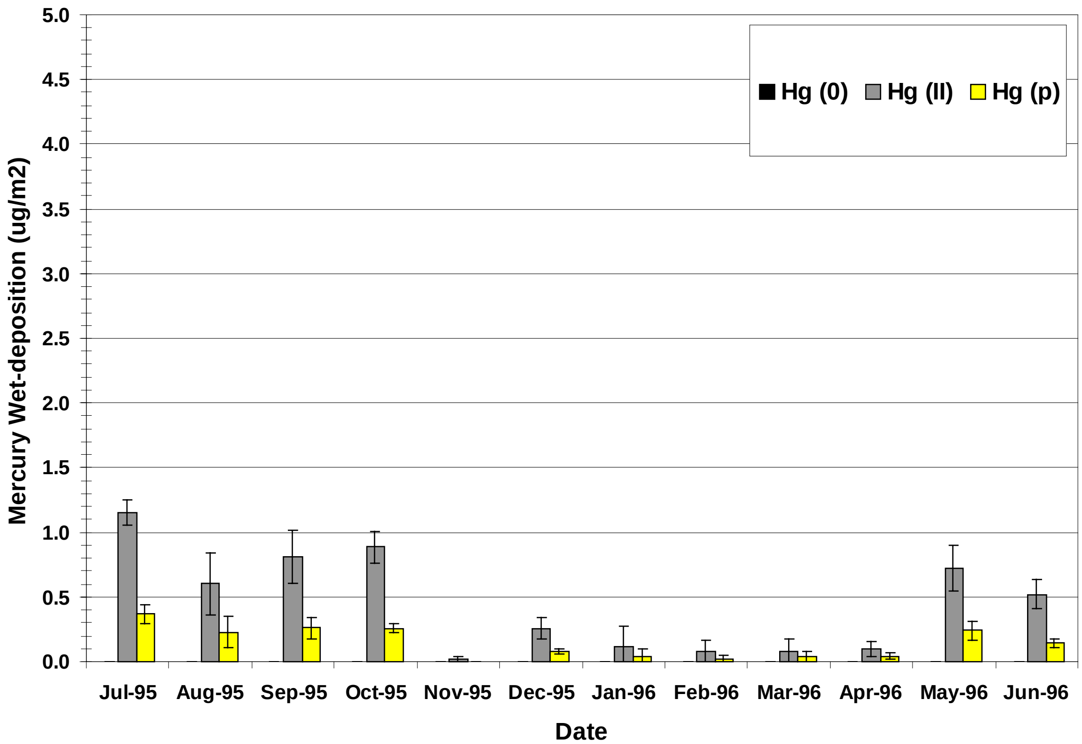

Figure 15. Modeled monthly speciated mercury wet-deposition to SFWMD WCA3 for Scenario #3.

<u>Model Estimates of the Monthly Dry-deposition of Speciated Mercury to the SFWMD WCA3</u>

The hybrid model estimates of the dry-deposition of mercury to the SFWMD WCA3 were performed for the same three emissions scenarios employed in the wet-deposition modeling exercise. The results for each of the three dry-deposition modeling scenarios are presented below. All dry-deposition estimates are presented in tabular form in Appendix D.

<u>Scenario #1: BASE CASE</u>

The hybrid model's estimate for the total mercury dry-deposition to SFWMD WCA3 during the one-year study period was 12.2 ± 7.4 $\mu g/m^2$. Monthly estimates of the total mercury dry-deposition to the SFWMD WCA3 are presented in Figure 16. While considerable variability exists in the monthly deposition estimates, inspection of Figure

16 indicates that on average, dry-deposition to the site does show a seasonal trend, with relatively greater deposition occurring during the climatological wet season. The general trends noted in the total mercury dry-deposition can be seen in Figure 17, as well. Figure 17 presents the results for the speciated dry-deposition of mercury to SFWMD WCA3. As was the case for the wet-deposition to SFWMD WCA3, dry-deposition to this area is dominated by the Hg(II) fraction.

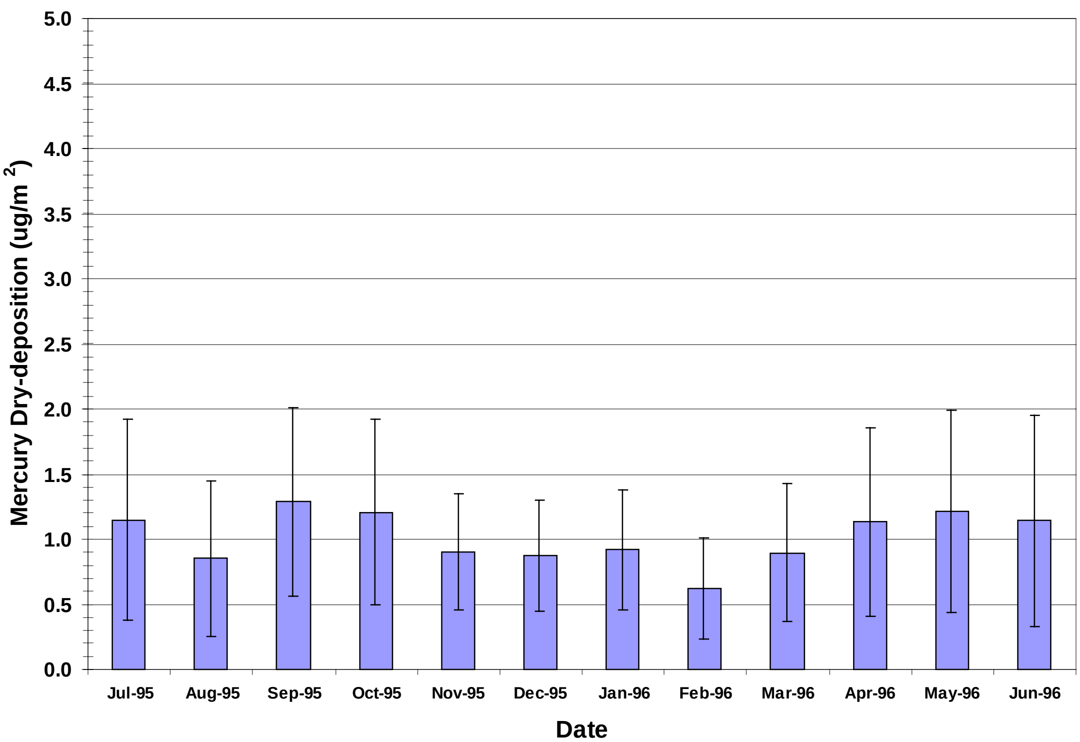

Figure 16. Modeled monthly total mercury dry-deposition to SFWMD WCA3 for Scenario #1.

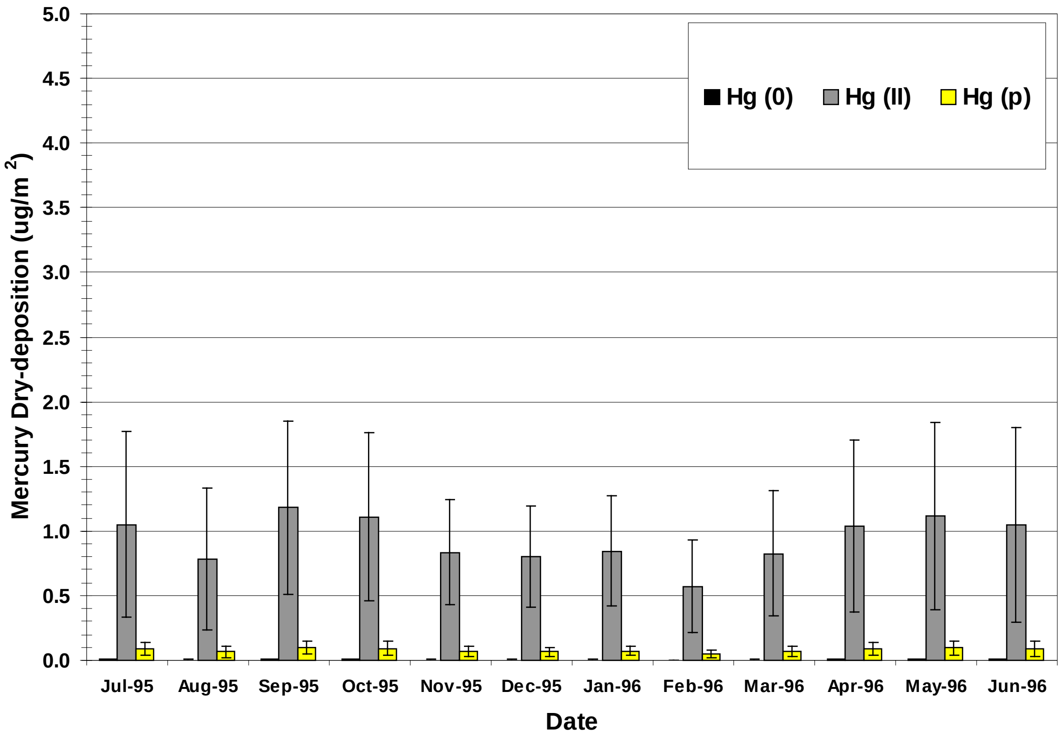

Figure 17. Modeled monthly speciated mercury dry-deposition to SFWMD WCA3 for Scenario #1.

Scenario #2

The hybrid model's estimate for the total mercury dry-deposition to SFWMD WCA3 (Scenario #2) during the one-year study period was 7.3 ± 3.8 $\mu g/m^2$, approximately 60 percent of the total mercury dry-deposition to the SFWMD WCA3 estimated under Scenario #1. The monthly estimates of the total mercury dry-deposition to the SFWMD WCA3 are presented in Figure 18. As was true for the Scenario #1 estimates, one can see that, on average, there is a seasonal trend in the estimated dry-deposition to the area.

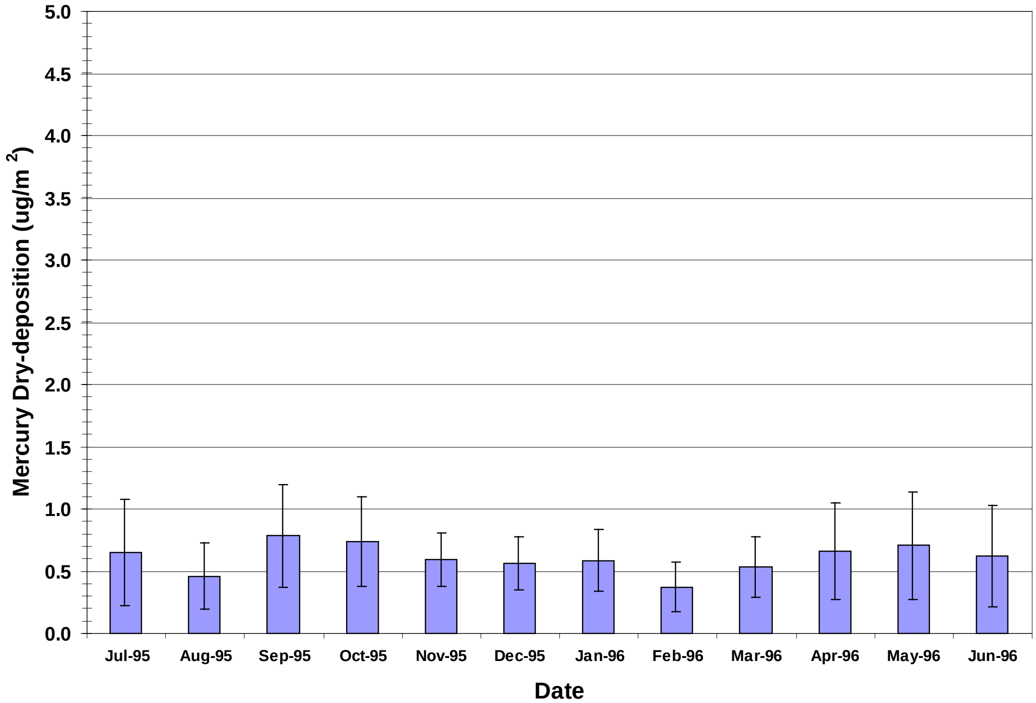

Figure 18. Modeled monthly total mercury dry-deposition to SFWMD WCA3 for Scenario #2.

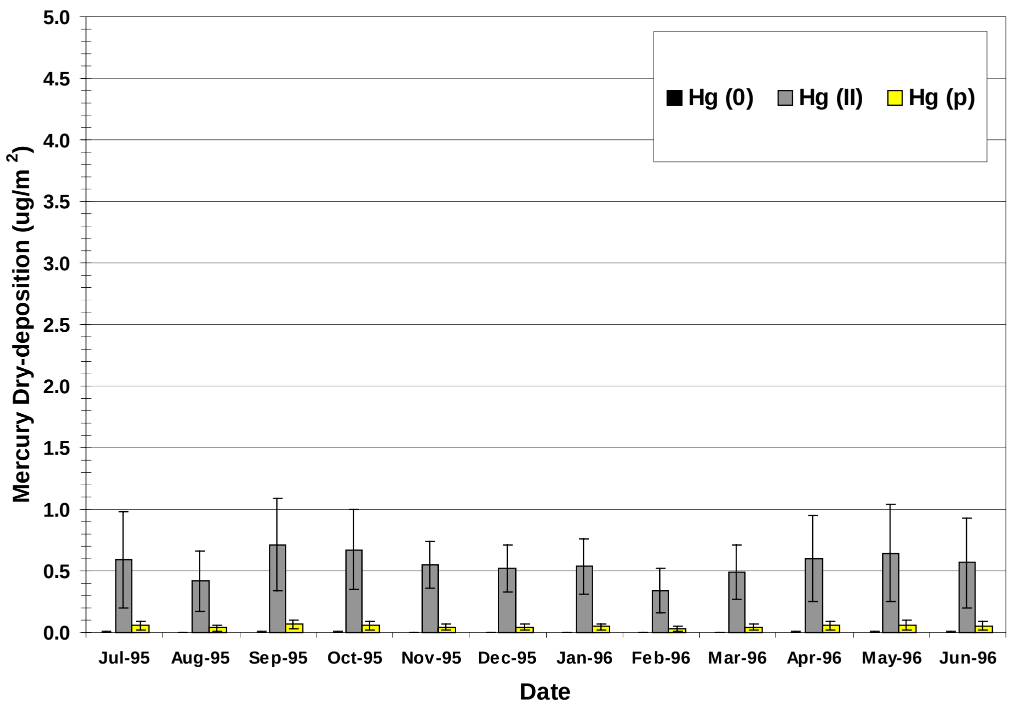

Figure 19. Modeled monthly speciated dry-deposition to SFWMD WCA3 for Scenario #2.

The speciated mercury dry-deposition estimates from Scenario #2 are presented in Figure 19. From this figure, it can be seen that once again, dry-depositional loading from Hg(II) dominates the total mercury deposition to WCA3.

Scenario #3

The hybrid model's estimate for the total mercury dry-deposition to SFWMD WCA3 (Scenario #2) during the one-year study period was 4.1 ± 2.1 $\mu g/m^2$. This total represents one-third of the total mercury dry-depositional loading estimated under Scenario #1. Monthly estimates of the total mercury dry-deposition to WCA3 are presented in Figure 20. Again, while some trend is noted in the data, the uncertainty placed on these estimates is large enough to suggest that this trend may not be statistically significant.

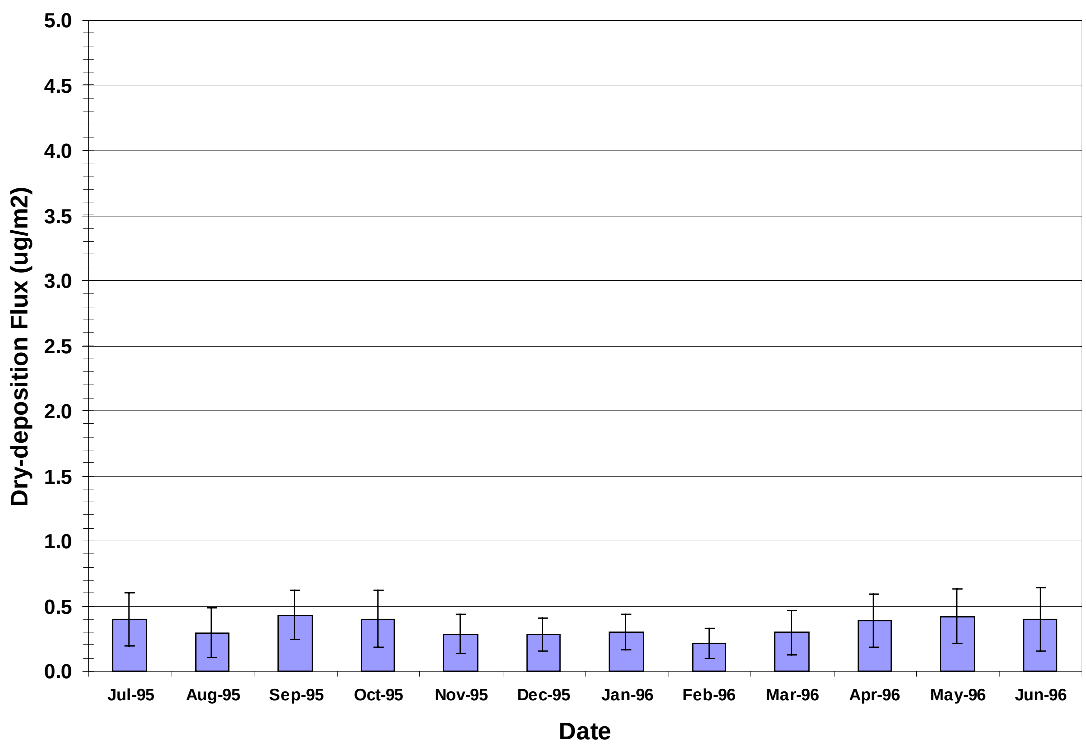

Figure 20. Modeled monthly total mercury dry-deposition to SFWMD WCA3 for Scenario #3.

In Figure 21, it can be seen that the reactive gaseous species of mercury, Hg (II), continues to be the dominant species contributing to the total mercury dry-deposition under Scenario #3, accounting for roughly 90 percent of the total dry-deposition.

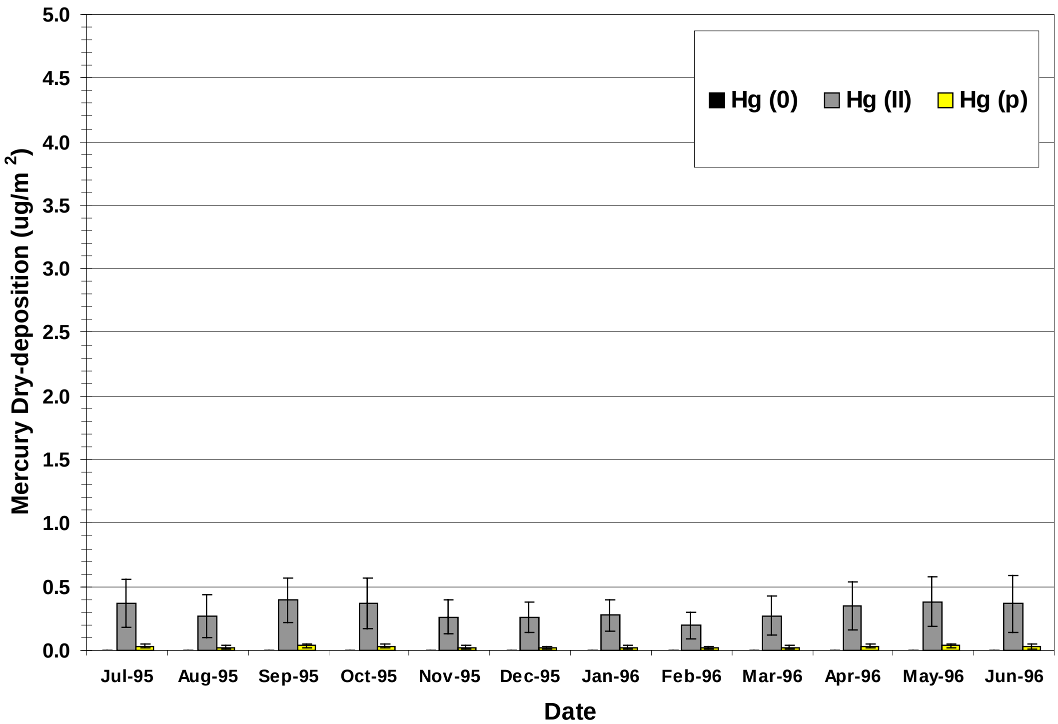

Figure 21. Modeled monthly speciated mercury dry-deposition to SFWMD WCA3 for Scenario #3.

5. Summary

For this project, a hybrid modeling approach was used that incorporated a mesoscale meteorological model and a dispersion and deposition model to obtain estimates of the monthly and annual wet- and dry-deposition of speciated mercury [Hg(0), Hg(II) and Hg(p)] to the South Florida Water Conservation District's Water Conservation Area 3 (SFWMD WCA3). Daily back-trajectories were computed for the study period and then grouped into eight, statistically distinct clusters which represented eight meteorologically distinct atmospheric transport regimes that impacted South Florida during the one-year period studied. Days representative of each of the meteorological clusters were modeled to obtain high-resolution meteorological fields which are then used to obtained cluster average estimates of speciated mercury wet- and dry-deposition fluxes. These cluster averages were weighted by the monthly frequency of occurrence of each cluster to obtain the monthly and annual deposition estimates for the one-year period studied. The monthly and annual estimates were performed for three emission scenarios in an effort to better understand how changes in local mercury emissions might impact future wet- and dry-depositional loading of mercury to the SFWMD WCA3. In addition, model sensitivity analyses were performed and presented. Uncertainties in the meteorological conditions within a few of the identified clusters resulted in relatively large uncertainties in the monthly estimates for WCA3 but were less important when looking at the annual deposition estimates. As expected, the dry deposition estimates were found to be sensitive to the deposition velocities used. Overall, the estimated values for WCA3 were in good agreement with the measured wet deposition values from the FAMS project. The model estimates also agreed quite well with the dry deposition estimates obtained during the 1999 FEDDS project where the first actual dry deposition measurements were made in the Everglades near the Water Management Districts S-151 structure. Considering the statistical nature of the modeling approach, the estimates presented appear to be quite reasonable. A considerably more comprehensive model is needed to more precisely define the deposition to South Florida and WCA3 that would require speciated Hg emissions data from each of the major sources in South Florida. Based upon the emissions inventory provided to us from the USEPA, local sources accounted for the majority (>95%) of the wet deposition regardless of the uncertainties in the modeling approach. Local sources also accounted for the majority (>85%) of the dry deposition to WCA3 with a slightly larger uncertainty in the estimates due to the model sensitivity to the dry deposition velocities, and the meteorological flow conditions used. Clearly more field measurements are needed to bound the dry deposition estimates and to provide better empirical relationships to be utilized in the comprehensive model development.

6. Acknowledgements

The authors would like to thank Dr. Tom Atkeson of the Florida Department of Environmental Protection and Mr. Kenneth P. Larson of the Broward County Department of Natural Resource Protection for their efforts in the collection of the precipitation data used in this report. We would like to thank Mr. Christopher Gleason for his assistance in the data analysis associated with this project. Finally, we would also like to thank Dr. Curt Pollman, TetraTech, for providing precipitation chemistry data from the Florida Atmospheric Mercury Study for use in stages of this work.

7. References

Brook, J.R., P.J. Samson and S. Sillman, 1995: Aggregation of three-day periods to estimate annual and seasonal wet-deposition totals for sulfate, nitrate and acidity. Part I: A synoptic and chemical climatology for Eastern North America. *J. of Appl. Meteor*., **34**, 297-325. c

Bullock, Jr., O. R., W. G. Benjey and M. H. Keating, 1997: Modeling of regional scale atmospheric mercury transport and deposition using RELMAP. Atmospheric Deposition of Contaminants to the Great Lakes and Coastal Waters: Joel E. Baker, Ed. pp.323-347.SETAC Press, Pensacola, Florida.

Dorling, S.R., T.D. Davies and C.E. Pierce, 1992a: Cluster analysis: a technique for estimating the synoptic meteorological controls on air and precipitation chemistry – method and applications. *Atmospheric Environment*, **26A**, 2575-2581.

Dorling, S.R., T.D. Davies and C.E. Pierce, 1992b: Cluster analysis: a technique for estimating the synoptic meteorological controls on air and precipitation chemistry – results from Eskdalemuir, South Scotland. *Atmospheric Environment*, **26A**, 2583-2602.

Dorling, S.R. and T.D. Davies, 1995: Extending cluster analysis-synoptica meteorology links to characterise chemical climates at six northwest European monitoring stations. *Atmospheric Environment*, **29**, 145-167.

Draxler, R.R., and A.D. Taylor, 1982. Horizontal dispersion parameters for long-range transport modeling. *J. Appl. Meteorol*., 21, 367-372.

Draxler, R.R. and G.D. Hess, 1997: Description of the HYSPLIT_4 Modeling System. NOAA TECHNICAL MEMORANDUM ERL ARL-224.

Dvonch, JT (1998): Utilization of event precipitation data to establish source-receptor relationships for mercury deposited in South Florida. *Ph.D. Dissertation, The University of Michigan.*

Dvonch, J.T., J.R. Graney, F.J. Marsik, G.J. Keeler and R.K. Stevens (1998): An investigation of source-receptor relationships for mercury in South Florida using event precipitation data. *Sci. Total Environ*. **213**, 95-108.

Dvonch, J.T., J.R. Graney, G.J. Keeler and R.K. Stevens (1999): Use of Elemental Tracers to Source Apportion Mercury in South Florida Precipitation. *Environ. Sci. Technol*. **33**, 4522-4527.

Eastman, J. L., and R.A. Pielke (1995): Comparison of Lake-Breeze Model Simulations with Tracer Data. *J. Appl. Meteor*., 34, 1398-1418.

Fernau, M.E. and P.J. Samson, 1990: Use of cluster analysis to define periods of similar meteorology and precipitation chemistry in Eastern North America. Part I: Transport patterns. *J. of Appl. Meteor*., **29**, 735-750,

Guentzel, J.L., W.M. Landing, G.A. Gill and C.D. Pollman, 1995: Atmospheric deposition of mercury in Florida: The FAMS Project (1992-1994). *Water, Air and Soil Pollut.*, **80**, 393-402.

Hicks, B.B., 1986: Differences in wet and dry particle deposition parameters between North America and Europe. *In Aerosols: Research, Risk Assessment, and Control Strategies*, Lewis Publishers, Chelsea, MI, 973-982.

Lyons, W.A., C.J. Tremback, R.A. Pielke (1995a): Applications of the Regional Atmospheric Modeling System (RAMS) to Provide Input to Photochemical Grid Models for the Lake Michigan Ozone Study (LMOS). *J. Appl. Meteor*., 34, 1762-1786.

Lyons, W.A., R.A. Pielke, C.J. Tremback, R.L. Walko, D.L. Moon, C.S. Keen (1995b): Modeling Impacts of Mesoscale Vertical Motions Upon Coastal Zone Air Pollution Dispersion. *Atmos. Environ,* 29, 283-301.

Moody, J.L. and P.J. Samson, 1989: The influence of atmospheric transport on precipitation chemistry at two sites in the midwestern United States. *Atmospheric Environment*, **23**, 2117-2132.

Pielke, R.A, R.T. McNider, M. Segal and Y. Mahrer, 1983: The use of a mesoscale numerical model for evaluations of pollutant transport and diffusion in coastal regions and over irregular terrain. *Bull. of the Amer. Me*teor. Soc., **64**, 243-249.

Shannon, J.D. and E.C. Voldner, 1995: Modeling of atmospheric concentrations of mercury and deposition to the Great Lakes. . *Atmospheric Environment*, **29**, No. 14, 1649-1661.

US EPA, 1997: Mercury Study Report to Congress, Volume II: An inventory of anthropogenic mercury emissions in the United States. EPA/452/R-9/003, December 1997. Research Triangle Park, NC.

Ward, J.H., 1963: Hierarchical grouping to optimize an objective function. *J of the American Statistical Association*, 236-244.

APPENDIX A

ATMOSPHERIC BACK-TRAJECTORIES BY CLUSTER

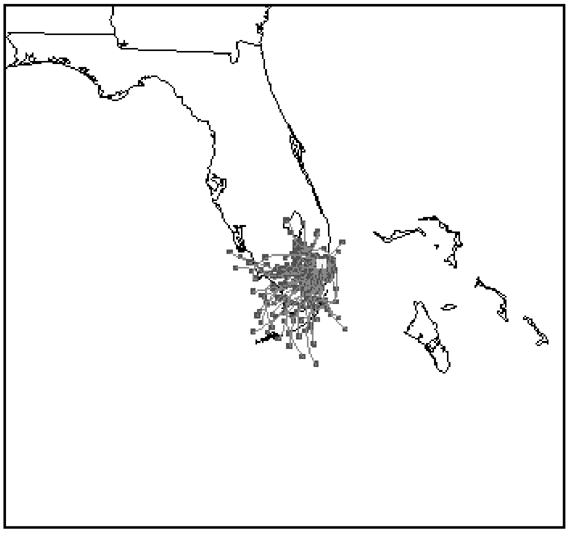

Figure A1. Cluster 1: Weak local flow, variable in direction, generally associated with a weak high pressure center located over South Florida.

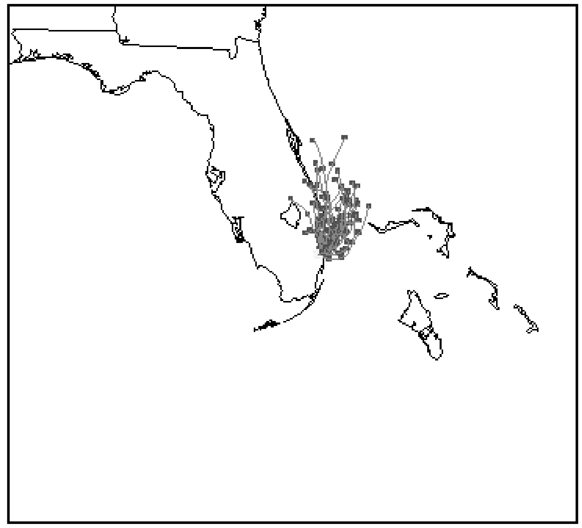

Figure A2. Cluster 2: Weak synoptic flow, northerly in direction, generally associated with both weak high and low pressure systems.

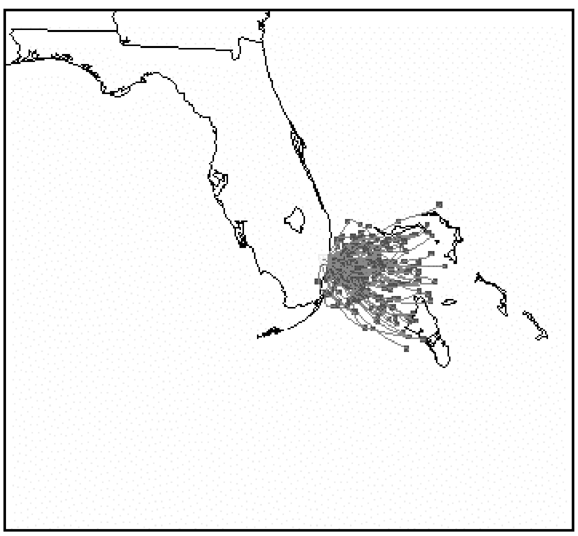

Figure A3. Cluster 3: Weak synoptic or enhanced sea-breeze flow, easterly in direction, generally associated with the influence of the Bermuda High.

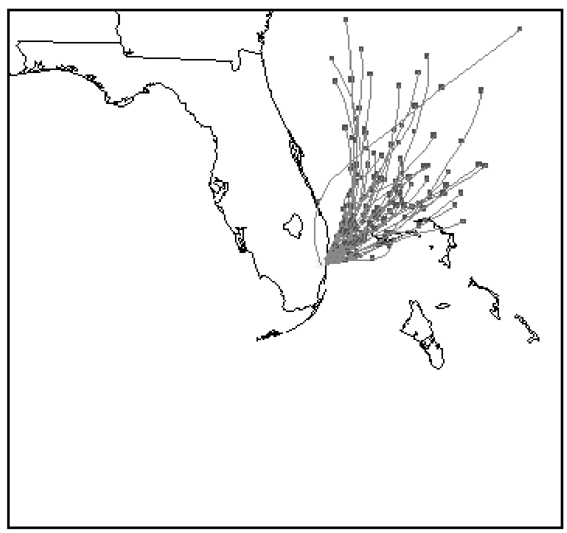

Figure A4. Cluster 4: Strong synoptic flow, northeasterly in direction, generally associated with strong high pressure over eastern U.S.

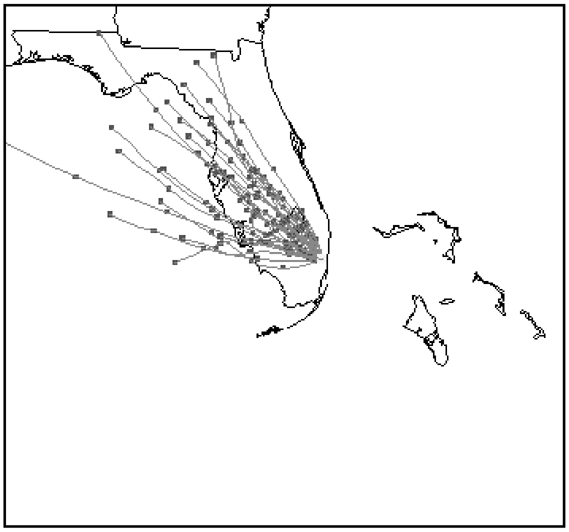

Figure A5. Cluster 5: Strong synoptic flow, northwesterly in direction, generally associated with the advance of a strong southern Plains high pressure area after a cold frontal passage.

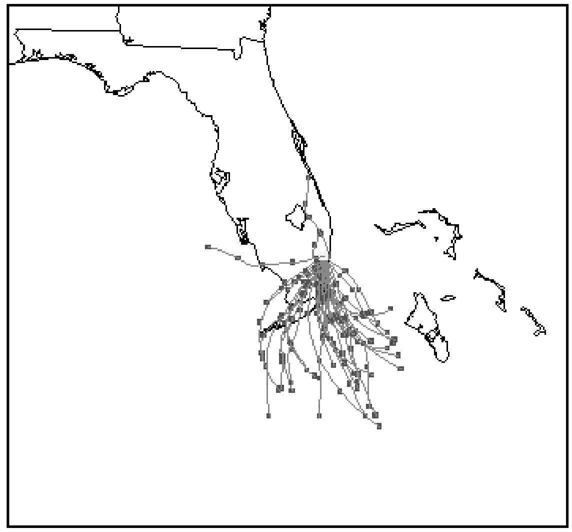

Figure A6. Cluster 6: Moderate synoptic flow, southerly in direction, generally associated with the approach of a cold frontal boundary from the northwest.

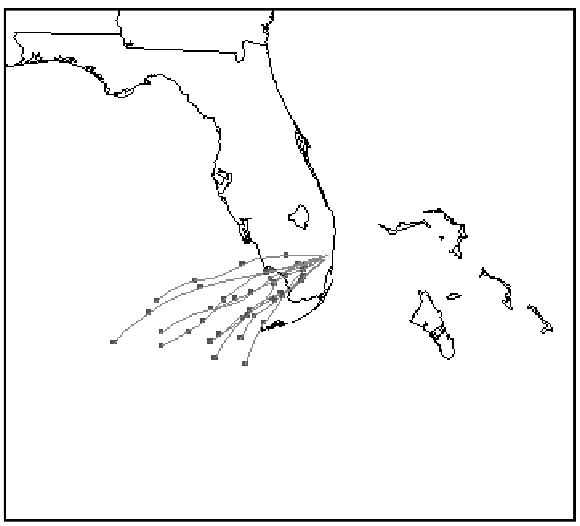

Figure A7. Cluster 7: Moderate synoptic flow, west to southwesterly in direction, generally associated with the weak troughs or multiple frontal boundaries.

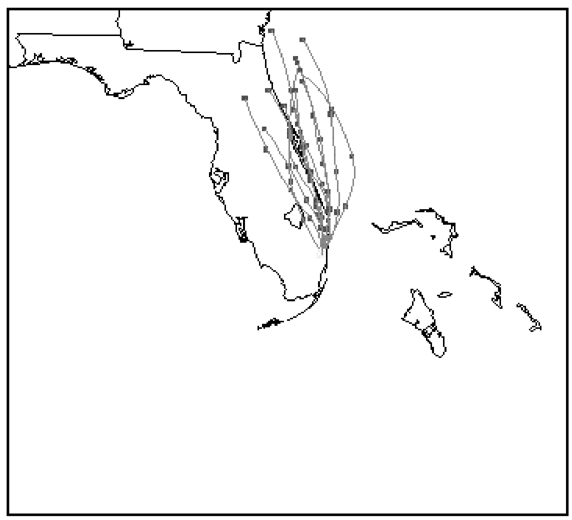

Figure A8. Cluster 8: Moderate to strong synoptic flow, north to northwesterly in direction, generally associated with strong high pressure areas in central and southern Plains.

APPENDIX B

SURFACE WEATHER MAPS

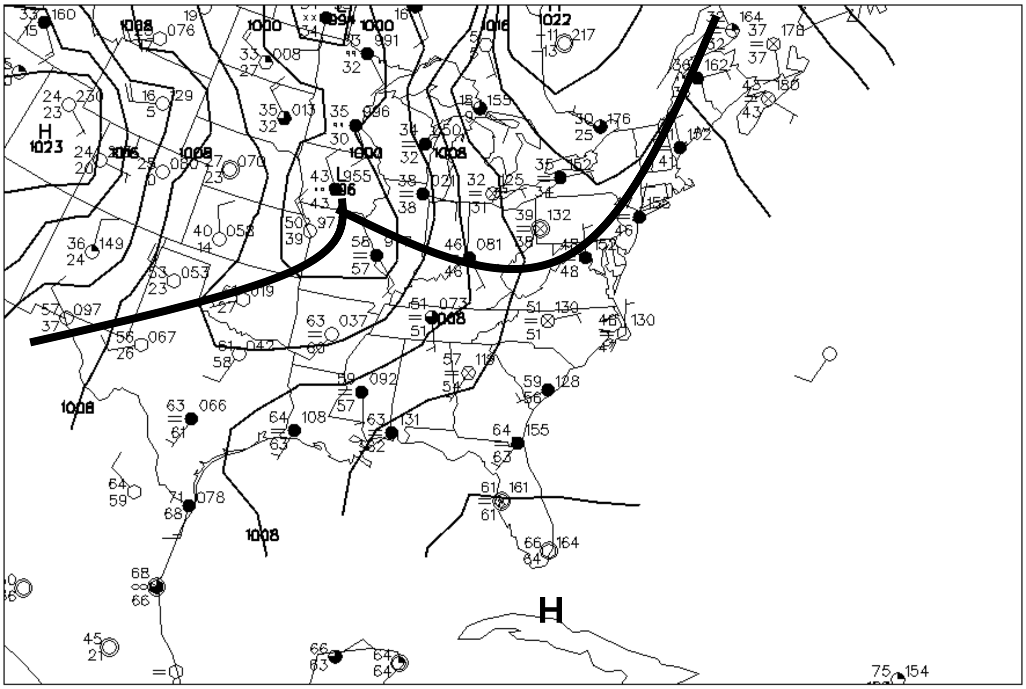

Plot of Surface Station data for 12Z 23 FEB 96

Figure B1. Surface map features representative of atmospheric transport associated with Cluster #1.

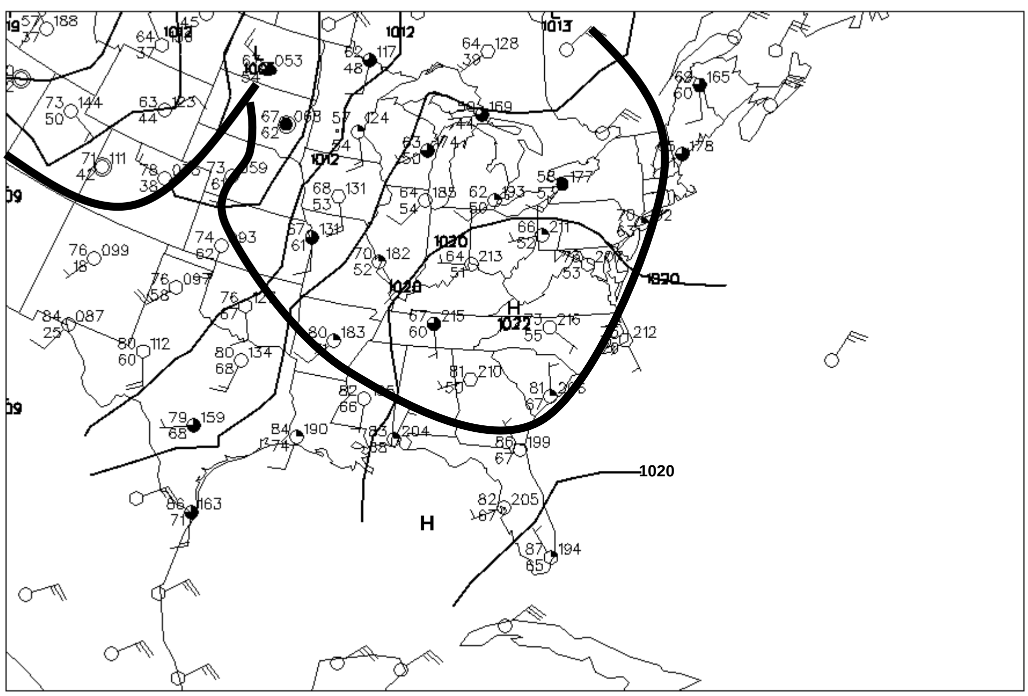

Plot of Surface Station data for 15Z 5 JUN 96

Figure B2. Surface map features representative of atmospheric transport associated with Cluster #2.

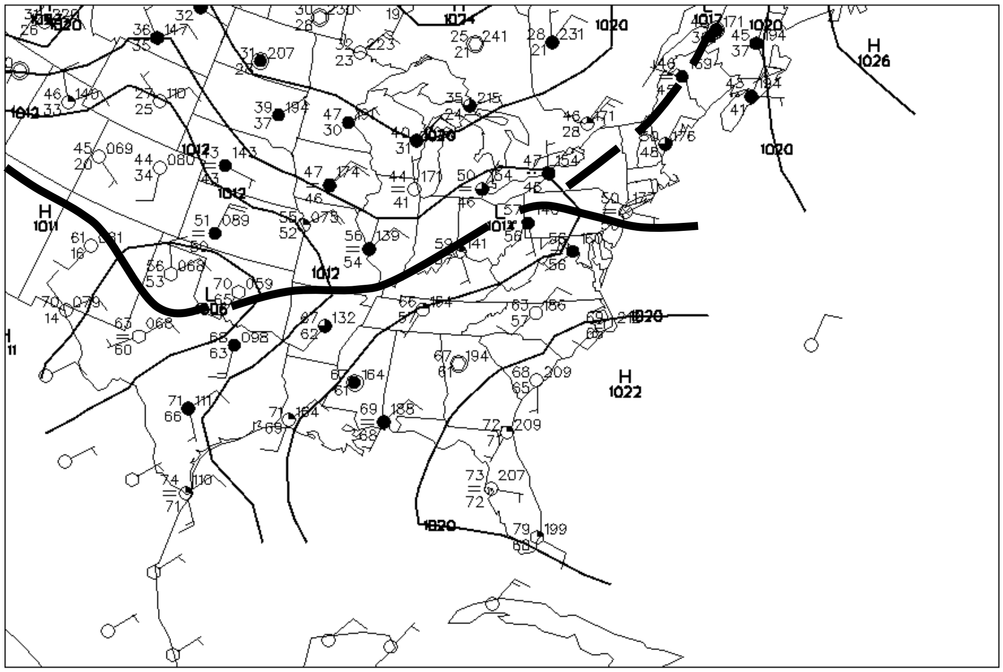

Plot of Surface Station data for 12Z 4 MAY 96

Figure B3. Surface map features representative of atmospheric transport associated with Cluster #3.

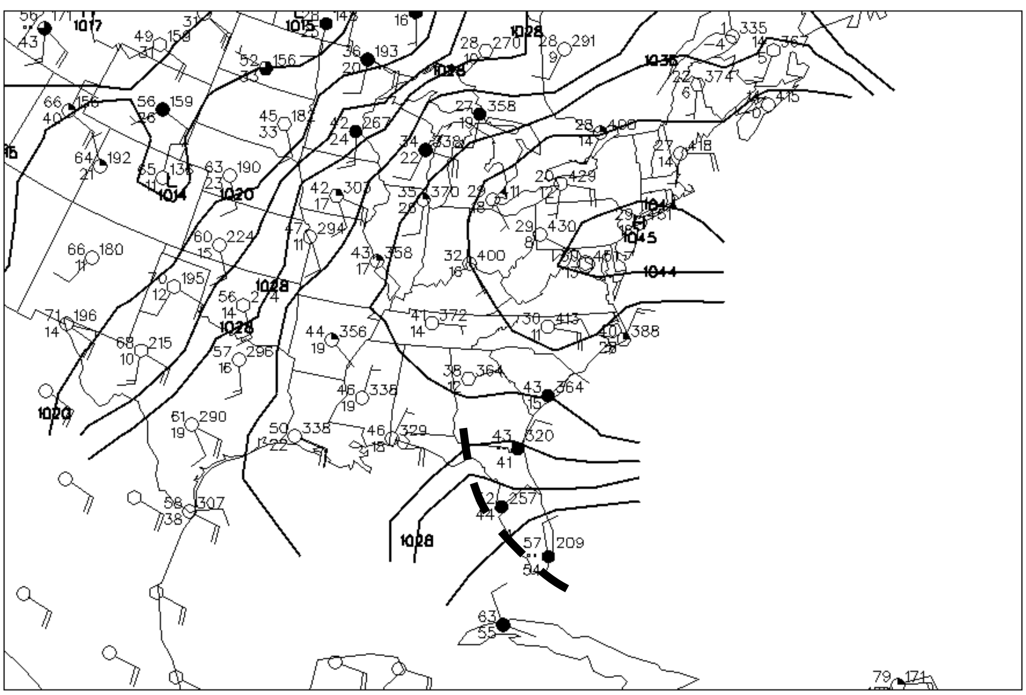

Plot of Surface Station data for 0Z 11 MAR 96

Figure B4. Surface map features representative of atmospheric transport associated with Cluster #4.

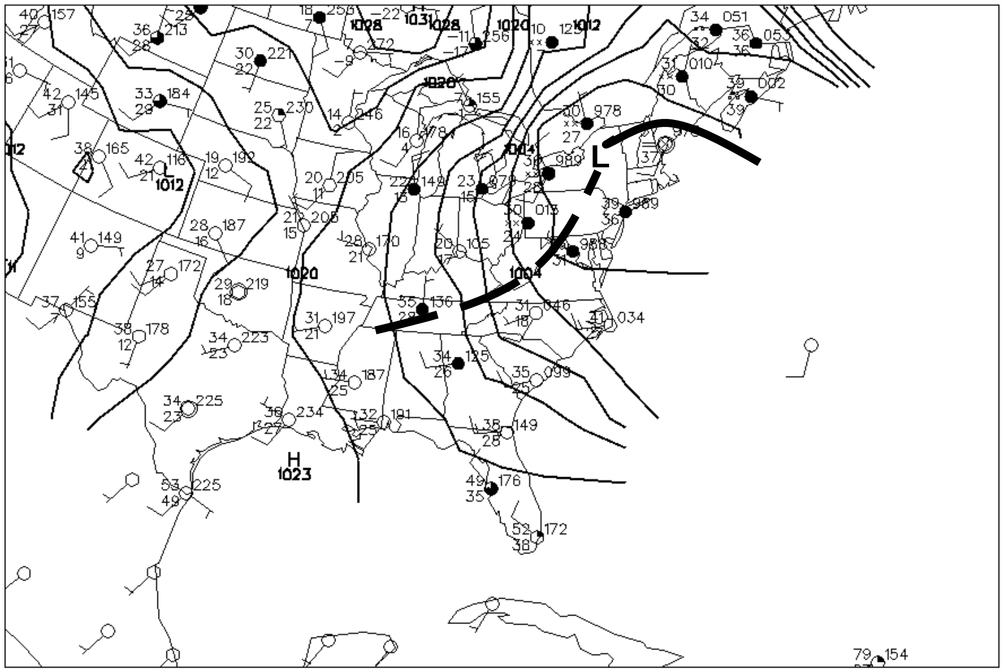

Figure B5. Surface map features representative of atmospheric transport associated with Cluster #5.

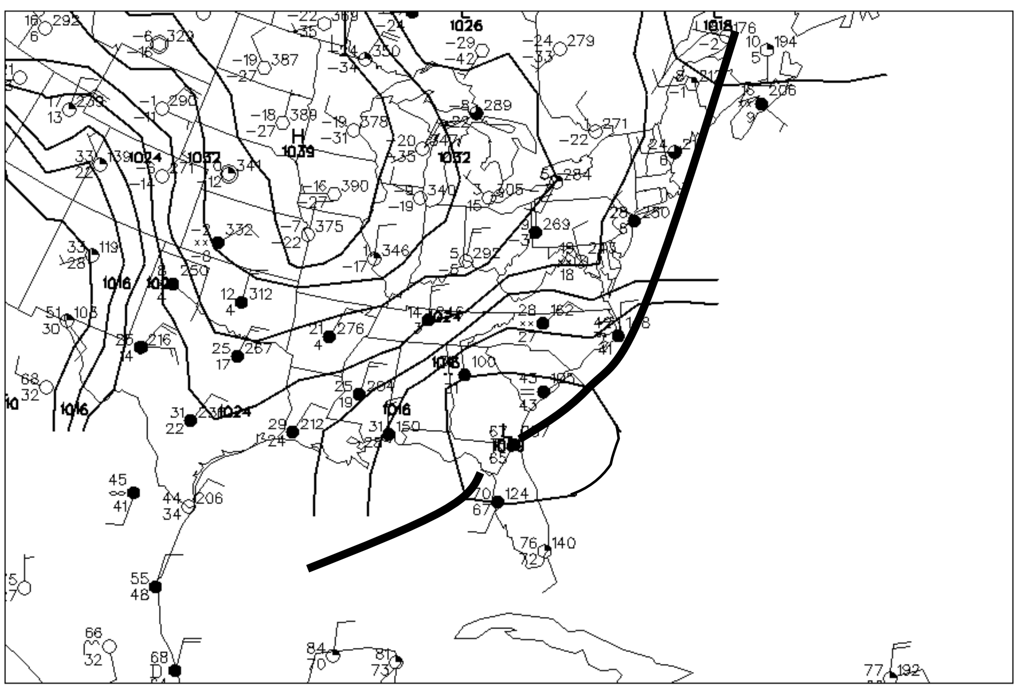

Figure B6. Surface map features representative of atmospheric transport associated with Cluster #6.

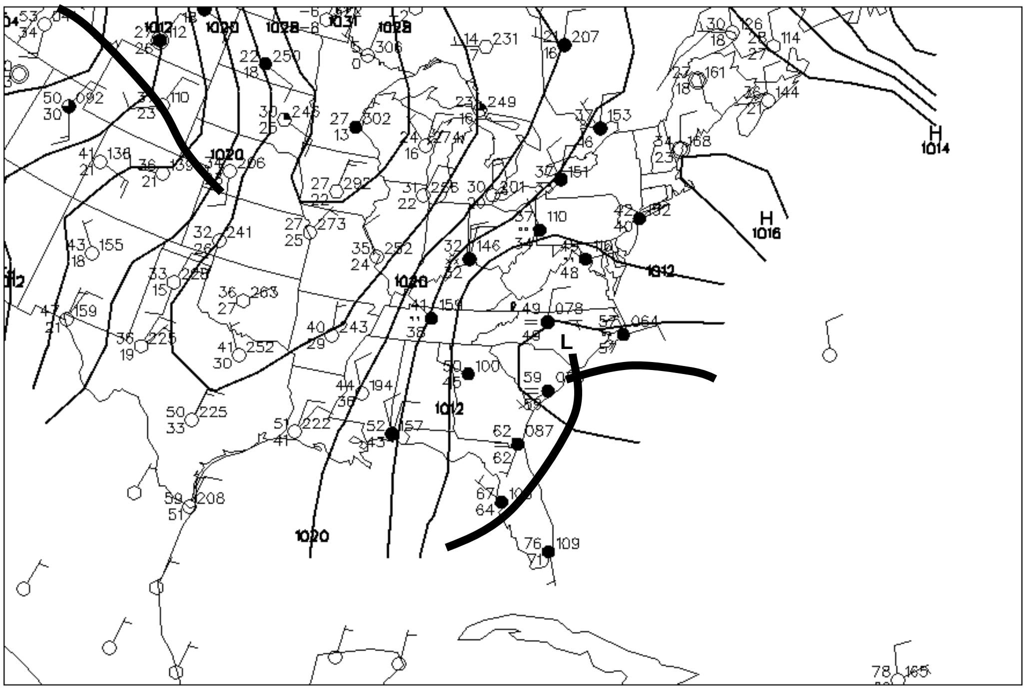

Plot of Surface Station data for 12Z 1 APR 96

Figure B7. Surface map features representative of atmospheric transport associated with Cluster #7.

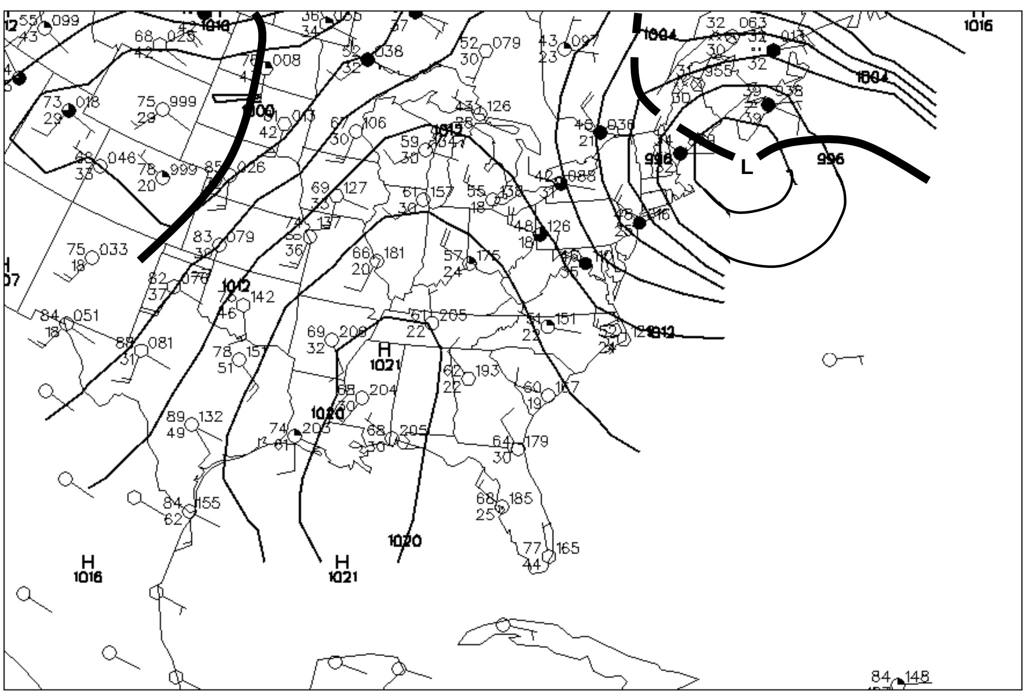

Plot of Surface Station data for 21Z 10 APR 96

Figure B8. Surface map features representative of atmospheric transport associated with Cluster #8.

APPENDIX C

MERCURY EMISSIONS INVENTORY FOR BASE CASE

TABLE C1. Local Source Emissions Employed in Hybrid Modeling (BASE CASE)

Lat	Lon	Stack Height (m)	Hg(II) (Fraction of Total)	HgO (Fraction of Total)	HgP (Fraction of Total)	Total Hg Emissions (ng/hr)	Site Type or Name
25.63	-80.30	46	0.30	0.50	0.20	121467.00	util_gas
26.05	-80.22	46	0.30	0.50	0.20	317791.00	util_gas
26.09	-80.13	105	0.30	0.50	0.20	1819962.00	util_gas
26.61	-80.07	38	0.30	0.50	0.20	41553.00	util_gas
25.44	-80.33	122	0.30	0.50	0.20	1182097.00	util_gas
26.07	-80.20	46	0.30	0.50	0.20	6141552.00	util_oil
26.09	-80.13	105	0.30	0.50	0.20	831689472.00	util_oil
26.61	-80.07	38	0.30	0.50	0.20	32796804.00	util_oil
25.44	-80.33	122	0.30	0.50	0.20	370570752.00	util_oil
25.80	-80.30	50	0.73	0.02	0.25	606685248.00	mwi_apc1237 225Health South Larkin General Hospital Miami
26.16	-81.80	50	0.73	0.02	0.25	798270080.00	mwi_apc1237 233Naples Community Hospital Naples FL
26.57	-80.08	50	0.73	0.02	0.25	66884476.00	mwi_apc4569 207John F. Kennedy Memorial Hospital Atlantis FL
26.35	-80.11	50	0.73	0.02	0.25	60278536.00	mwi_apc4569 210Boca Raton Community Hospital Boca Raton
25.66	-80.36	50	0.73	0.02	0.25	66058676.00	mwi_apc4569 211Baptist Hospital of Miami Dade FL
25.80	-80.30	50	0.73	0.02	0.25	1054913728.00	mwi_apc4569 212MedX Inc. Dade County
26.62	-81.88	50	0.73	0.02	0.25	116989272.00	mwi_apc4569 214Lee Memorial Hospital Fort Myers FL
26.02	-80.19	50	0.73	0.02	0.25	176958576.00	mwi_apc4569 217Hollywood Memorial Hospital Hollywood FL
25.79	-80.20	50	0.73	0.02	0.25	196620544.00	mwi_apc4569 226Jackson Memorial Hospital Miami FL
25.73	-80.24	50	0.73	0.02	0.25	74316096.00	mwi_apc4569 227Mercy Hospital Miami FL
25.85	-80.21	50	0.73	0.02	0.25	61930020.00	mwi_apc4569 228North Shore Hospital Miami FL
25.70	-80.30	50	0.73	0.02	0.25	150414720.00	mwi_apc4569 229South Miami Hospital Miami FL
25.78	-80.24	50	0.73	0.02	0.25	172043040.00	mwi_apc4569 230V.A. Med. Ctr-Miami Miami FL
25.82	-80.13	50	0.73	0.02	0.25	197848416.00	mwi_apc4569 231Miami Beach Community Hospital Miami Beach FL
26.66	-80.09	50	0.73	0.02	0.25	28263128.00	mwi_apc4569 248V.A. Center Palm Beach West Palm Beach FL
25.84	-80.36	75	0.60	0.20	0.20	131976716288.00	munwaste Dade Co. RRF
26.18	-80.22	75	0.60	0.20	0.20	64248516608.00	munwaste Broward Co. RRF North
26.06	-80.24	75	0.60	0.20	0.20	64248516608.00	munwaste Broward Co. RRF South
25.80	-80.32	75	0.60	0.20	0.20	2309360896.00	munwaste Miami International Airport
25.46	-81.16	75	0.60	0.20	0.20	7104223744.00	munwaste Southernmost WTE
25.84	-80.33	75	0.30	0.50	0.20	4840544768.00	hgpoint 12025Pennsuco Cement Co.
25.77	-80.19	75	0.30	0.50	0.20	3338098176.00	hgpoint 12025Rinker Portland Cement Co.
26.15	-80.45	75	0.30	0.50	0.20	4988583936.00	boilers Broward FL 12011
26.08	-81.40	75	0.30	0.50	0.20	605022848.00	boilers Collier FL 12021
25.61	-80.50	75	0.30	0.50	0.20	7705480704.00	boilers Dade FL 12025
26.55	-81.17	75	0.30	0.50	0.20	102511424.00	boilers Hendry FL 12051
26.58	-81.92	75	0.30	0.50	0.20	1335616512.00	boilers Lee FL 12071
25.12	-81.15	75	0.30	0.50	0.20	310502304.00	boilers Monroe FL 12087
26.64	-80.44	75	0.30	0.50	0.20	3436072960.00	boilers Palm Beach FL 12099

APPENDIX D

SUMMARY OF MONTHLY SPECIATED WET- AND DRY-DEPOSITION ESTIMATES FOR THE SOUTH FLORIDA WATER MANAGEMENT DISTRICT'S WATER CONSERVATION AREA 3

TABLE D1. Hybrid Model Estimates and Uncertainties for Wet-deposition to SFWMD WCA Using Scenario #1 Emissions.
All units are in micrograms per square meter.

	Total Hg	Total Hg Unc.	Hg (0)	Hg (0) Unc.	Hg (II)	Hg (II) Unc	Hg (p)	Hg (p) Unc.
Jan-96	0.43	0.60	0.00	0.00	0.32	0.45	0.11	0.15
Feb-96	0.27	0.34	0.00	0.00	0.21	0.27	0.05	0.07
Mar-96	0.30	0.41	0.00	0.00	0.21	0.29	0.08	0.12
Apr-96	0.39	0.20	0.00	0.00	0.29	0.15	0.10	0.05
May-96	2.56	0.75	0.00	0.00	1.95	0.54	0.60	0.21
Jun-96	1.77	0.47	0.00	0.00	1.40	0.38	0.36	0.10
Jul-95	3.98	0.61	0.00	0.00	3.04	0.39	0.94	0.22
Aug-95	2.23	1.11	0.00	0.00	1.67	0.77	0.56	0.34
Sep-95	2.83	0.87	0.00	0.00	2.17	0.62	0.66	0.24
Oct-95	3.02	0.47	0.00	0.00	2.36	0.37	0.66	0.10
Nov-95	0.05	0.05	0.00	0.00	0.05	0.04	0.00	0.00
Dec-95	0.93	0.28	0.00	0.00	0.73	0.23	0.20	0.05
Annual Totals	**18.74**	**6.15**	**0.01**	**0.00**	**14.40**	**4.51**	**4.33**	**1.65**

TABLE D2. Hybrid Model Estimates and Uncertainties for Wet-deposition to SFWMD WCA Using Scenario #2 Emissions.
All units are in micrograms per square meter.

	Hg(T)	Hg (T) Unc.	Hg (0)	Hg (0) Unc.	Hg (II)	Hg (II) Unc	Hg (p)	Hg (p) Unc.
Jan-96	0.26	0.36	0.00	0.00	0.19	0.27	0.07	0.09
Feb-96	0.15	0.20	0.00	0.00	0.12	0.15	0.04	0.05
Mar-96	0.17	0.23	0.00	0.00	0.12	0.16	0.05	0.07
Apr-96	0.18	0.10	0.00	0.00	0.12	0.07	0.06	0.03
May-96	1.41	0.42	0.00	0.00	1.05	0.29	0.36	0.13
Jun-96	0.95	0.20	0.00	0.00	0.74	0.15	0.21	0.05
Jul-95	2.24	0.32	0.00	0.00	1.69	0.20	0.55	0.11
Aug-95	1.08	0.46	0.00	0.00	0.77	0.30	0.31	0.16
Sep-95	1.63	0.52	0.00	0.00	1.23	0.37	0.40	0.15
Oct-95	1.75	0.32	0.00	0.00	1.34	0.24	0.41	0.08
Nov-95	0.02	0.02	0.00	0.00	0.02	0.02	0.00	0.00
Dec-95	0.47	0.13	0.00	0.00	0.35	0.10	0.12	0.04
Annual Totals	**10.31**	**3.28**	**0.00**	**0.00**	**7.74**	**2.31**	**2.57**	**0.97**

TABLE D3. Hybrid Model Estimates and Uncertainties for Wet-deposition to SFWMD WCA Using Scenario #3 Emissions.
All units are in micrograms per square meter.

	Hg(T)	Hg (T) Unc.	Hg (0)	Hg (0) Unc.	Hg (II)	Hg (II) Unc	Hg (p)	Hg (p) Unc.
Jan-96	0.16	0.21	0.00	0.00	0.12	0.16	0.04	0.05
Feb-96	0.10	0.12	0.00	0.00	0.08	0.09	0.02	0.03
Mar-96	0.12	0.14	0.00	0.00	0.08	0.10	0.04	0.04
Apr-96	0.14	0.08	0.00	0.00	0.10	0.06	0.04	0.02
May-96	0.96	0.25	0.00	0.00	0.72	0.18	0.24	0.08
Jun-96	0.67	0.15	0.00	0.00	0.52	0.11	0.14	0.03
Jul-95	1.52	0.17	0.00	0.00	1.15	0.10	0.37	0.07
Aug-95	0.83	0.36	0.00	0.00	0.60	0.24	0.23	0.12
Sep-95	1.07	0.29	0.00	0.00	0.81	0.20	0.26	0.09
Oct-95	1.14	0.16	0.00	0.00	0.88	0.13	0.26	0.03
Nov-95	0.02	0.02	0.00	0.00	0.02	0.02	0.00	0.00
Dec-95	0.34	0.10	0.00	0.00	0.26	0.08	0.08	0.02
Annual Totals	**7.07**	**2.07**	**0.00**	**0.00**	**5.34**	**1.47**	**1.72**	**0.60**

TABLE D4. Hybrid Model Estimates and Uncertainties for Dry-deposition to SFWMD WCA for Using Scenario #1 Emissions. All units are in micrograms per square meter.

	Total Hg	Total Hg Unc.	Hg (0)	Hg (0) Unc.	Hg (II)	Hg (II) Unc	Hg (p)	Hg (p) Unc.
Jan-96	0.92	0.46	0.00	0.00	0.84	0.43	0.07	0.03
Feb-96	0.62	0.39	0.00	0.00	0.57	0.36	0.05	0.03
Mar-96	0.90	0.53	0.00	0.00	0.82	0.48	0.07	0.04
Apr-96	1.13	0.72	0.01	0.00	1.04	0.67	0.09	0.05
May-96	1.21	0.78	0.01	0.00	1.11	0.72	0.10	0.05
Jun-96	1.14	0.81	0.01	0.00	1.05	0.75	0.09	0.06
Jul-95	1.15	0.77	0.01	0.00	1.05	0.72	0.09	0.05
Aug-95	0.85	0.60	0.00	0.00	0.78	0.55	0.06	0.04
Sep-95	1.29	0.72	0.01	0.00	1.18	0.67	0.10	0.05
Oct-95	1.21	0.71	0.01	0.00	1.11	0.65	0.09	0.06
Nov-95	0.91	0.45	0.00	0.00	0.83	0.41	0.07	0.04
Dec-95	0.87	0.42	0.00	0.00	0.80	0.39	0.07	0.03
Annual Totals	**12.20**	**7.37**	**0.06**	**0.03**	**11.20**	**6.80**	**0.94**	**0.53**

TABLE D5. Hybrid Model Estimates and Uncertainties for Dry-deposition to SFWMD WCA for Using Scenario #2 Emissions. All units are in micrograms per square meter.

	Total Hg	Total Hg Unc.	Hg (0)	Hg (0) Unc.	Hg (II)	Hg (II) Unc	Hg (p)	Hg (p) Unc.
Jan-96	0.59	0.25	0.00	0.00	0.54	0.22	0.05	0.02
Feb-96	0.37	0.20	0.00	0.00	0.34	0.18	0.03	0.02
Mar-96	0.53	0.24	0.00	0.00	0.49	0.22	0.04	0.02
Apr-96	0.66	0.38	0.00	0.00	0.60	0.35	0.06	0.04
May-96	0.71	0.43	0.00	0.00	0.64	0.39	0.06	0.04
Jun-96	0.62	0.40	0.00	0.00	0.57	0.37	0.05	0.04
Jul-95	0.65	0.43	0.00	0.00	0.59	0.39	0.06	0.04
Aug-95	0.46	0.27	0.00	0.00	0.42	0.25	0.04	0.02
Sep-95	0.78	0.41	0.00	0.00	0.71	0.38	0.07	0.04
Oct-95	0.73	0.36	0.00	0.00	0.67	0.32	0.06	0.04
Nov-95	0.60	0.21	0.00	0.00	0.55	0.19	0.04	0.02
Dec-95	0.57	0.21	0.00	0.00	0.52	0.19	0.04	0.02
Annual Totals	**7.26**	**3.80**	**0.04**	**0.02**	**6.63**	**3.45**	**0.59**	**0.36**

TABLE D6. Hybrid Model Estimates and Uncertainties for Dry-deposition to SFWMD WCA for Using Scenario #3 Emissions. All units are in micrograms per square meter.

	Total Hg	Total Hg Unc.	Hg (0)	Hg (0) Unc.	Hg (II)	Hg (II) Unc	Hg (p)	Hg (p) Unc.
Jan-96	0.30	0.13	0.00	0.00	0.27	0.12	0.02	0.01
Feb-96	0.21	0.11	0.00	0.00	0.19	0.10	0.02	0.01
Mar-96	0.30	0.17	0.00	0.00	0.27	0.15	0.02	0.01
Apr-96	0.39	0.21	0.00	0.00	0.35	0.19	0.03	0.02
May-96	0.42	0.21	0.00	0.00	0.38	0.19	0.03	0.02
Jun-96	0.40	0.24	0.00	0.00	0.36	0.22	0.03	0.02
Jul-95	0.40	0.20	0.00	0.00	0.37	0.19	0.03	0.01
Aug-95	0.30	0.19	0.00	0.00	0.27	0.17	0.02	0.01
Sep-95	0.43	0.19	0.00	0.00	0.39	0.17	0.04	0.01
Oct-95	0.40	0.22	0.00	0.00	0.37	0.20	0.03	0.02
Nov-95	0.29	0.15	0.00	0.00	0.26	0.13	0.02	0.01
Dec-95	0.28	0.13	0.00	0.00	0.26	0.12	0.02	0.01
Annual Totals	**4.11**	**2.13**	**0.02**	**0.01**	**3.75**	**1.96**	**0.34**	**0.16**